



1988

Pressure-Solution Features of the Birdbear Formation (Devonian), Williston Basin, North Dakota

James C. Collier
University of North Dakota

Follow this and additional works at: <https://commons.und.edu/theses>

 Part of the [Geology Commons](#)

Recommended Citation

Collier, James C., "Pressure-Solution Features of the Birdbear Formation (Devonian), Williston Basin, North Dakota" (1988). *Theses and Dissertations*. 59.

<https://commons.und.edu/theses/59>

This Thesis is brought to you for free and open access by the Theses, Dissertations, and Senior Projects at UND Scholarly Commons. It has been accepted for inclusion in Theses and Dissertations by an authorized administrator of UND Scholarly Commons. For more information, please contact zeinebyousif@library.und.edu.

PRESSURE-SOLUTION FEATURES OF THE BIRDBEAR FORMATION
(DEVONIAN), WILLISTON BASIN, NORTH DAKOTA

by
James C. Collier

Bachelor of Science, New Mexico Institute of Mining and
Technology, 1985

A Thesis
Submitted to the Graduate Faculty
of the
University of North Dakota
in partial fulfillment of the requirements
for the degree of
Master of Science

Grand Forks, North Dakota

August
1988

Copyright by
James C. Collier

1988

ii

77988
C69

This Thesis submitted by James C. Collier in partial fulfillment of the requirements for the Degree of Master of Science from the University of North Dakota has been read by the Faculty Advisory Committee under whom the work has been done, and is hereby approved.

Howard J. Fisher

(Chairperson)

Don L. Halverson

Robert J. Stevenson

This Thesis meets the standards for appearance and conforms to the style and format requirements of the Graduate School of the University of North Dakota, and is hereby approved.

A. William Johnson 6/6/88

Dean of the Graduate School

Permission

Title Pressure-Solution Features of the Birdbear
Formation (Devonian), Williston Basin, North
Dakota

Department Geology and Geological Engineering

Degree Master of Science

In presenting this thesis in partial fulfillment of the requirements for a graduate degree from the University of North Dakota, I agree that the Library of this University shall make it freely available for inspection. I further agree that permission for extensive copying for scholarly purposes may be granted by the professor who supervised my thesis work or, in his absence, by the Chairman of the Department or the Dean of the Graduate School. It is understood that any copying or publication or other use of this thesis or part thereof for financial gain shall not be allowed without my written permission. It is also understood that due recognition shall be given to me and to the University of North Dakota in any scholarly use which may be made of any material in my thesis.

Signature

James C. Callot

Date

5-25-88

ACKNOWLEDGEMENTS

I would like to thank my committee members, Drs. H.J. Fischer, R.J. Stevenson, and D. Halvorson for their help in editing this thesis. Dr. Howard Fischer provided hours of helpful and interesting conversation about geology and the world. Dr. Robert Stevenson is acknowledged for providing a job in the Natural Materials Analytical Laboratory as well as a constant supply of jokes and bad puns. The graduate student community of the Department of Geology and Geological Engineering must be thanked for making the years of graduate school enjoyable. Finally, I would like to thank my wife Cindy for her unfaltering support and my parents for never giving up.

TABLE OF CONTENTS

ACKNOWLEDGEMENTS.....	iv
LIST OF ILLUSTRATIONS.....	vii
LIST OF TABLES.....	ix
ABSTRACT.....	x
INTRODUCTION.....	1
Purpose	
Location and Lithology	
PREVIOUS WORKS.....	5
Mechanisms of Pressure Solution	
Categorization of Pressure Solution and	
Associated Features	
Reactate Dolomite	
Methods	
Pressure-solution Terminology	
PRESSURE-SOLUTION RESPONSE.....	23
Introduction	
Description of Pressure-Solution Response	
Procedure and Data	
Discussion	
The influence of Depth on Pressure-Solution	
Response	
Host Rock Influence on Pressure-Solution	
Response	
MINERALOGIC CHANGES DUE TO PRESSURE SOLUTION.....	40
Introduction	
Reactate Dolomites	
Description	
Discussion	
Pre-dolomite setting	
Eogenetic processes	
Post-deposition and burial	
Mesogenetic Processes	
Magnesium sources	
Pressure solution	
Nucleation	
Crystal Growth	
The Resultant Reactate Dolomite	

The Relation Between Pressure Solution and Neomorphism

Procedure and Data
Description

Discussion

Affects of temperature and pressure on
Neomorphism
Influence of ions in the intercrystalline
fluids
Mesogenetic dolomite as magnesium sinks

CONCLUSIONS.....	70
APPENDICIES.....	73
Appendix A: Thin section description	
Appendix B: Morphologic data of stylolites	
Appendix C: Chemical data for reactate dolomite	
REFERENCES CITED.....	88

LIST OF ILLUSTRATIONS

Figure

1.	Map showing the location of the Williston Basin.....	2
2.	Regional map showing location of studied wells.....	3
3.	Weyl's (1959) solution film hypothesis.....	7
4.	The stylolite classification of Logan and Semeniuk (1976).....	10
5.	Diagrammatic representation of pressure-solution related features.....	11
6.	The pressure-solution seam terminology of Wanless (1979).....	12
7.	The pressure-solution seam classification scheme of Buxton and Sibley (1981).....	15
8.	The definition of the amplitude and wavelength of a stylolite.....	21
9.	Photomicrograph of a stylolite showing peaked and columnar morphologic forms.....	24
10.	Photomicrograph of a iden in a stylolite.....	24
11.	Photomicrograph of a solution seam.....	26
12.	Photomicrograph of a stylolite overprinting a solution seam.....	26
13.	Photomicrograph of a solution seam occurring at a textural inhomogeneity at the boundary between an fossil allochem and the muddy matrix.....	29
14.	A plot of stylolite amplitude versus the depth at which it occurred.....	34
15.	A plot of stylolite wavelength versus the depth at which it occurred.....	34
16.	A plot of wavelength versus amplitude.....	38

Figure

17.	A photomicrograph of a reactae dolomite rhomb.....	43
18.	A photomicrograph of a group of reactate dolomite along a solution seam.....	43
19.	A diagrammatic representation of the interaction volume of the electron beam with a reactate dolomite rhomb.....	46
20.	Diagrammatic representation of the pressure-solution sandwich and the origin of reactate dolomite.....	52
21.	Diagrammatic representation of crystal growth by screw dislocation.....	58
22.	Photomicrograph of point-source burial dolomite in a muddy matrix.....	67
23.	Diagrammatic view of the small-scale concentration gradient developed during mesogenetic dolomite formation.....	68

LIST OF TABLES

Tables

1	Size parameters for stylolites.....	32
2	The number and type of pressure-solution seam for each lithology present.....	37
3	The relation of neomorphism and pressure solution.....	61

ABSTRACT

Pressure-solution features of the Birdbear Formation (Devonian), Williston Basin, North Dakota were the subject of this study. In the area studied, the Birdbear Formation is primarily a limestone with mud-rich textures. The investigation contained three principal phases: 1) a study of the parameters influencing the size and shape of the pressure-solution response, 2) the process of reactate dolomite formation and its relation to calcite neomorphism, and 3) the relation of neomorphism to pressure solution.

The principal pressure-solution response types are stylolites and solution seams. Stylolites are pressure-solution seams with a tooth-and-socket, serrated shape. Pressure-solution seams are gently undulating to smooth in shape.

In the first phase of the study, the parameters judged to be the most important in determining the shape and size of the pressure-solution response were depth of burial, texture of the host rock, and the cementation history. The amount of change with depth in individual wells had no detectable influence on the pressure-solution response, whereas a weak relation of increasing amplitude with increasing depth was found between wells. Texturally, the packstones had more peaked pressure-solution seams than did the other limestone textures, and mudstones hosted

pressure-solution seams with the largest amplitudes. Because of the predominantly mud-rich textures of the samples, the role of cementation history in influencing pressure-solution response was difficult to determine.

The second phase of the study concentrated on the formation of reactate dolomite, dolomite that grows in or near a pressure-solution seam. It was deduced that the physical environment of the pressure-solution seam is ideally suited to the formation of reactate dolomite. This environment is in the form of a "pressure-solution sandwich" composed of two layers of host rock, surrounding two boundary layers of water, and both around a central layer of clay-rich insoluble residue. These components provide nucleation sites, diffusion pathways, and ion sources for the formation of reactate dolomite.

The relation between neomorphism and pressure solution is that they co-occur in a similar physico-chemical environment. In addition, reactate dolomite and another type of mesogenetic dolomite, point-source burial dolomite, can help propagate neomorphic calcite. The two dolomite types act as magnesium sinks, removing magnesium ions from the local fluid system allowing neomorphism to proceed.

INTRODUCTION

Purpose

The purpose of this study is to investigate the relation between pressure solution and its host rock. More specifically, the study concentrates on the influence of lithology on the style and size of pressure-solution features, as well as the influence of pressure solution on the host rock itself. This involved consideration of the growth of new minerals on or near the seam and the alteration of the rock by recrystallization.

Location and Lithology

The well cores used for this study were drilled from the Williston Basin of North Dakota. The Williston Basin is a tectonic basin located in the northeastern corner of Montana, northwestern South Dakota, western North Dakota, southwestern Manitoba and southeastern Saskatchewan (Fig. 1). The wells from which the studied cores were taken are located in McKenzie, Williams, Divide, Burke and Bottineau counties, North Dakota (Fig. 2). The cores are archived in the Wilson M. Laird Core and Sample Library of the North Dakota Geological Survey on the campus of the University of North Dakota, Grand Forks, North Dakota.

Location of the Williston Basin in Central North America

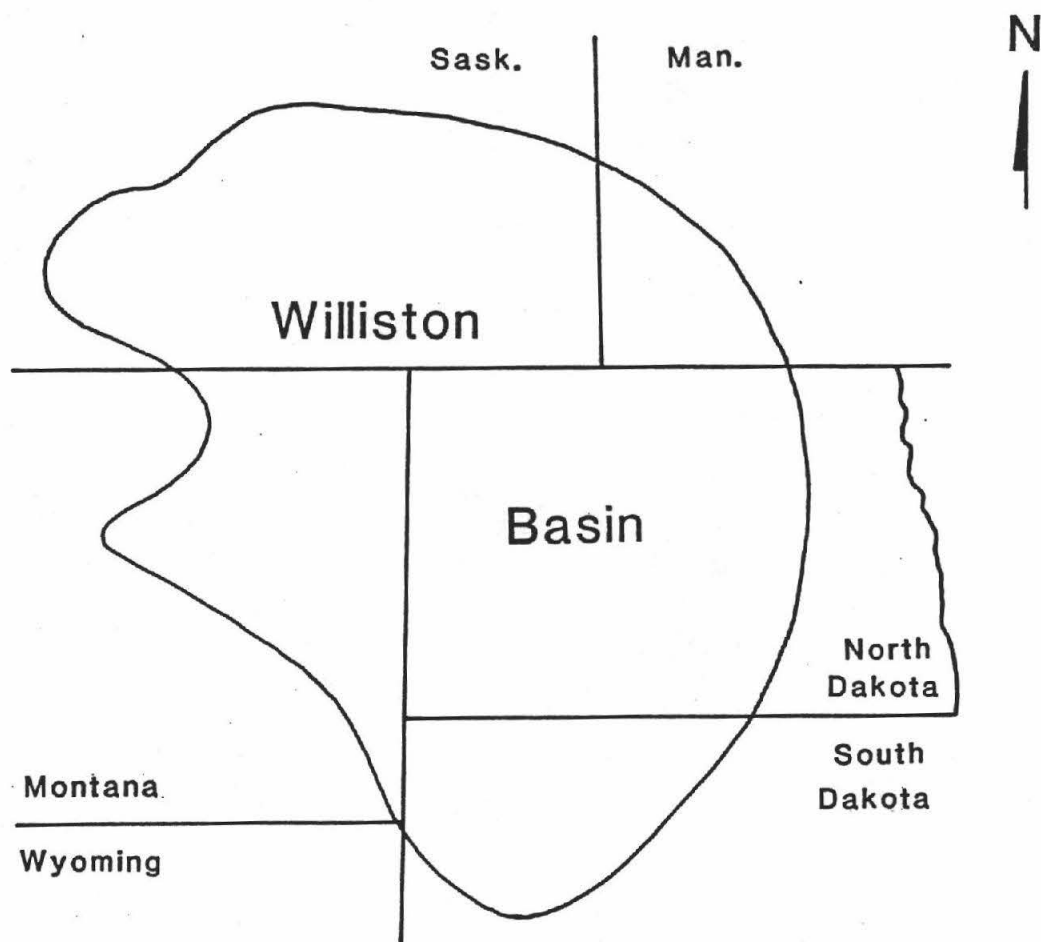


Figure 1: A regional map showing the location of the Williston Basin in relation to the states and provinces of central North America.

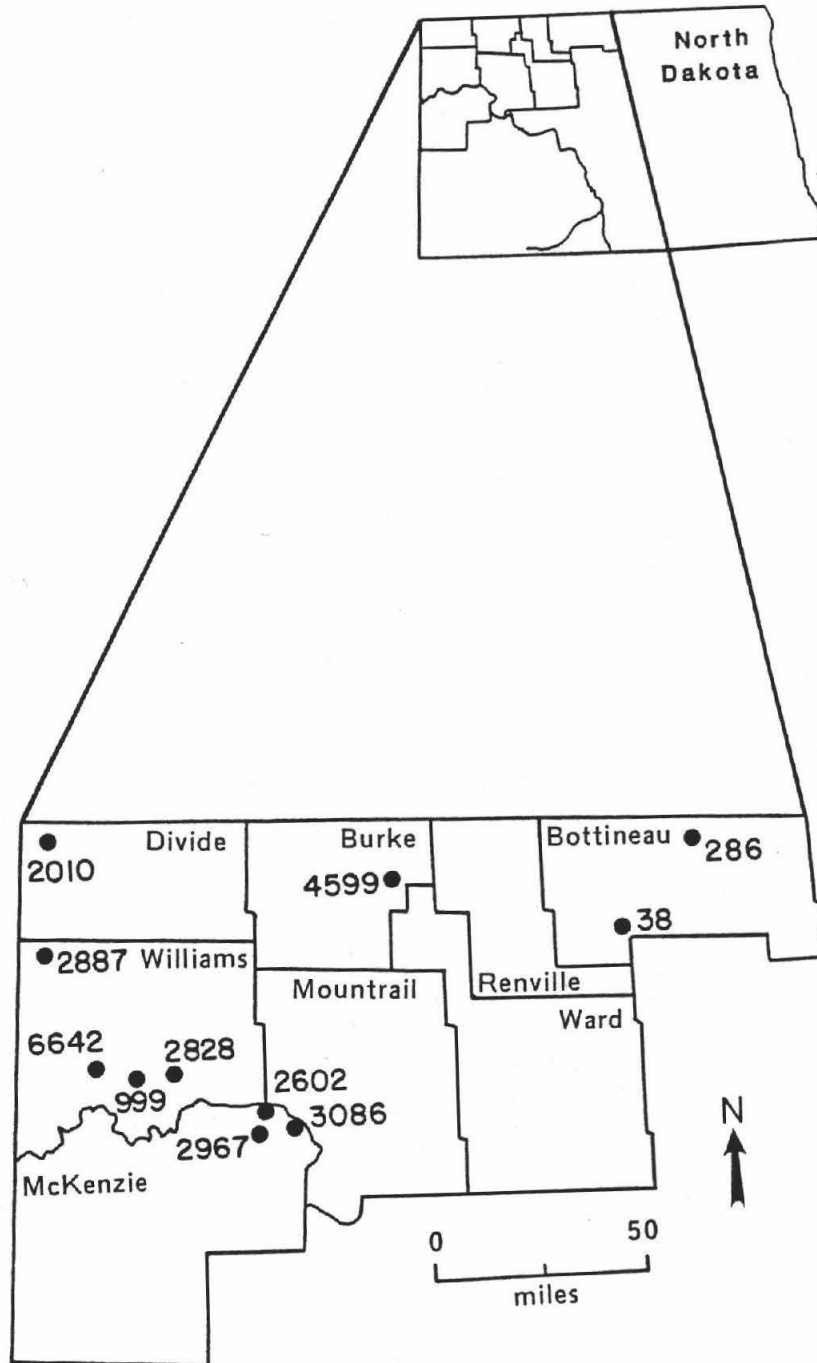


Figure 2: A regional map of northwestern North Dakota showing the location of the eleven wells used for this study. Each well is identified by its North Dakota Geologic Survey number.

All of the cores studied are from the Devonian Birdbear Formation. The samples are from most of the intervals described by Loeffler (1982). The present study uses Loeffler's (1982) descriptions and interpretations as a basis for lithologic classification and depositional environment determination for the studied section.

The Birdbear Formation is composed mostly of carbonate lithologies with common mudstone, wackestone and packstone and rare grainstone textures. Among these, the packstone and wackestone lithologies are the most abundant. The non-carbonate portion of the Birdbear occurs as enterolithic anhydrite in a dolo-mudstone that occurs at the top of the unit. Loeffler (1982) divides the Birdbear Formation into seven lithofacies. The sediments representing the lower portion of the Birdbear Formation were deposited in shallow, normal-marine conditions, with the middle Birdbear sediments originating from bank, back-bank, restricted shallow-water and supratidal conditions. By "late Birdbear time," sabkha conditions dominated the study area (Loeffler, 1982).

PREVIOUS WORKS

Mechanisms of Pressure Solution

The mechanisms that operate to facilitate the actual process of pressure solution are not widely pursued in modern geologic literature. Bathurst (1958, 1975) and Weyl (1959) presented two distinct models on the mechanisms of pressure solution that remain the basic models that later papers either support or dispute.

Bathurst's (1958, 1975) undercutting explanation of pressure solution requires pressure solution to occur at the micro- and/or macro-topographic irregularities of grain surface contacts. This would result in a network of interconnecting pores filled with solution at grain-to-grain contacts. This connected system of pores is necessary to ensure that a layer of solution exists between the two opposing grains. If the contact was strictly solid to solid, the ability of the system to transfer ions would cease, and pressure solution would stop.

Because of the need to maintain solution between the two surfaces, Bathurst later (1959, 1975) developed a multi-stage model referred to as the undercutting hypothesis (Weyl, 1959, Bathurst 1975). In the first stage of the undercutting hypothesis, the two surfaces meet at a point. Subsequently, pressure solution reduces the point,

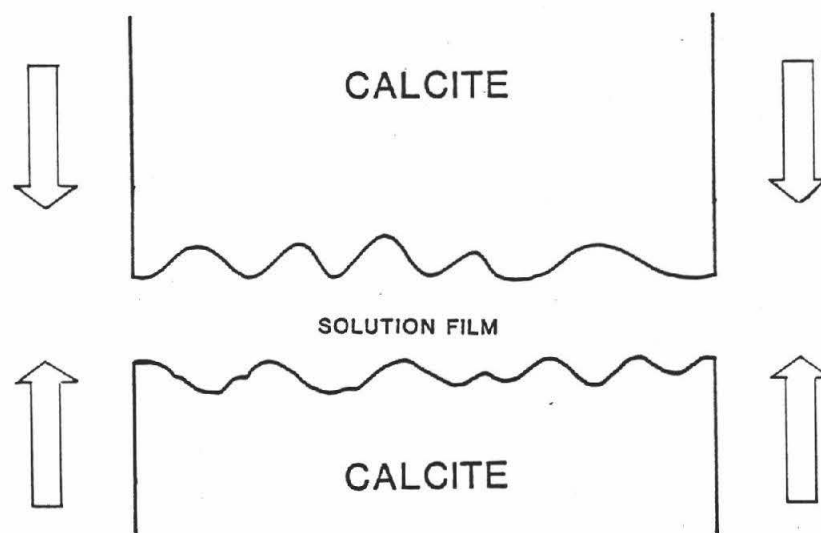
until the point of contact between the two grains is a surface. At this stage the contact is solid to solid, stopping the transfer of ions and pressure solution. But, at their edges, the strained crystal lattices of the grains are in contact with the solution that surrounds them. Ion transfer begins at these edges and the point contacts dissolve centripetally until a point is once more formed, beginning the cycle over again.

Bathurst (1975) admits that there are difficulties in explaining his undercutting model on the atomic level. Indeed, I have reviewed no later literature that used Bathurst's (1958, 1975) undercutting hypothesis. Bathurst (1975) himself admits that his model probably is not satisfactory, although it is not totally dismissed.

Shortly after the publication of Bathurst's (1958) model, Weyl (1959) introduced his solution film hypothesis to explain pressure solution (Fig. 3). Weyl (1959) based his model on indirect experimental results and rigorous mathematical treatment.

Weyl's (1959) ideas on the process of pressure solution were stimulated by the experiments of Becker and Day (1916) and Taber (1916) in which they demonstrated that a growing crystal could lift an inert mass placed upon it. From observing the effectiveness of the force of crystallization (Weyl, 1959, Bathurst, 1975), Weyl

SOLUTION FILM HYPOTHESIS



(AFTER WEYL, 1959)

Figure 3: Diagrammatic representation of the solution film hypothesis of Weyl (1959). Between the opposing calcite crystal surfaces there must exist a solution film of water that can support a shear stress.

concluded three important points: (1) a solution film must be maintained between a growing crystal and its constraint, (2) the solution film must be able to support a shear stress, so it does not act mechanically as a liquid, and (3) while not acting mechanically as a liquid, it must allow the diffusion of ions through it. On the basis of these three points Weyl (1959) developed a general equation for the transport of solute by diffusion and a very complete mathematical treatment of pressure solution and the force of crystallization.

The solution film hypothesis of Weyl (1959) is widely accepted and supported by many later works on pressure solution (Logan and Semeniuk, 1976, DeBoer, 1977, Wanless, 1979, Buxton and Sibley, 1981). Bathurst's (1959, 1975) undercutting model lacks the indirect experimentation and mathematical rigor of Weyl's (1959) solution film hypothesis. Weyl's (1959) model was used as a framework during this research project.

Categorization of Pressure Solution and Associated Features

The process of pressure solution leaves symptomatic signs in the host rock. These symptoms of pressure solution can be generally referred to as pressure-solution seams. The seams can be divided into two more specific categories based on seam shape; solution seams and stylolites (Wanless, 1979, Buxton and Sibley, 1981). Solution seams are wavy to smooth in shape, and can be of any size. Stylolites are tooth and socket interdigitations that are usually peaked or flat topped in form, and can also be of any size (Logan and Semeniuk, 1976, Wanless, 1979).

According to Stockdale (1922) the earliest mention of stylolites was in 1751 by Mylius who described them as Schwielen. The term "stylolite" was not coined until 1828

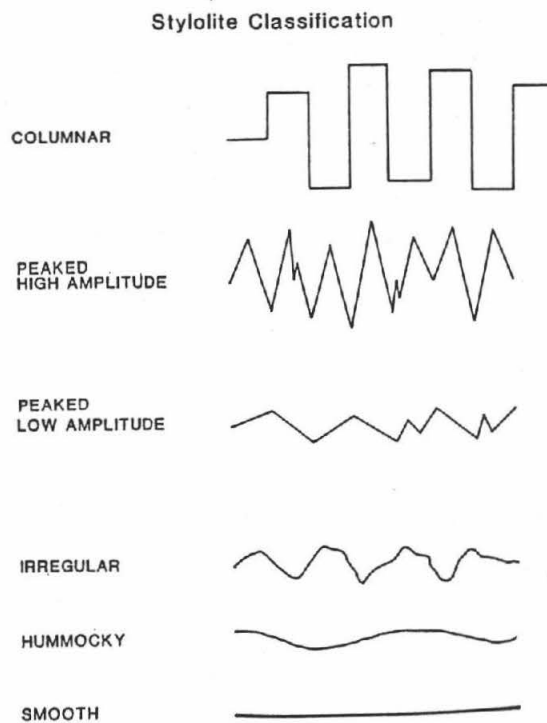
when Kloden described stylolite traces as a distinct fossil taxon named Stylolithes sulcata. Even though Kloden was incorrect in calling it a fossil, the term stylolite continues to be used in the geologic literature, because of its usefulness as a descriptive term.

Since the time of Mylius, many writers have considered the subject of stylolites. Sorby (1879) was the first to suggest a solution theory for the origin of stylolites. Stockdale (1923, 1943) gives a very useful review of the early workers, plus very detailed descriptions of the shapes and occurrences of stylolites. Dunnington (1954) argues for the post-induration solution origin of stylolites, rebuking earlier arguments against the post-induration solution origin of stylolites.

The recent pressure-solution literature begins with Logan and Semeniuk's (1976) work in the Canning Basin of Australia. Their contribution includes the definition of several terms that are very useful when discussing pressure solution. They also list five stylolite shape categories: hummocky to smooth, irregular, peaked low-amplitude, peaked high-amplitude, and flat-topped columnar (Fig. 4). Among these types, they state that the hummocky to smooth and irregular types are the most common. This first serious attempt to categorize pressure-solution features was based solely upon morphology, and did not attempt to infer genetic associations as did later studies (Wanless, 1979,

Buxton and Sibley, 1981).

In describing the basic components of stylolites, Logan and Semeniuk (1976) present three new terms: iden, stylocummulate and reactate (Fig. 5). The word iden is taken from the Latin, meaning "the body of the same" and is defined by Logan and Semeniuk (1976, p.8) as, "a body of material that behaves as a statistically homogeneous unit under a set of specific physical and chemical conditions: it is a finitely extended body independent of scale, geometry and composition."



(FROM LOGAN & SEMENIUK, 1976)

Figure 4: The stylolite classification of Logan and Semeniuk (1976) illustrating its morphological basis.

Wanless (1979) documents the basic types of pressure-solution features in limestones and shows how they relate to certain types of dolomites. He delineated three types of pressure-solution features: (1) sutured-seam (2) non-sutured seam, and (3) non-seam solution-dolomitization (Fig. 6).

The first type, the suture seam, has the typical, saw-tooth stylolite morphology. Wanless suggested that this type of response formed in limestone units that are structurally resistant to stress and contain little or no

Pressure-Solution Seam Terminology

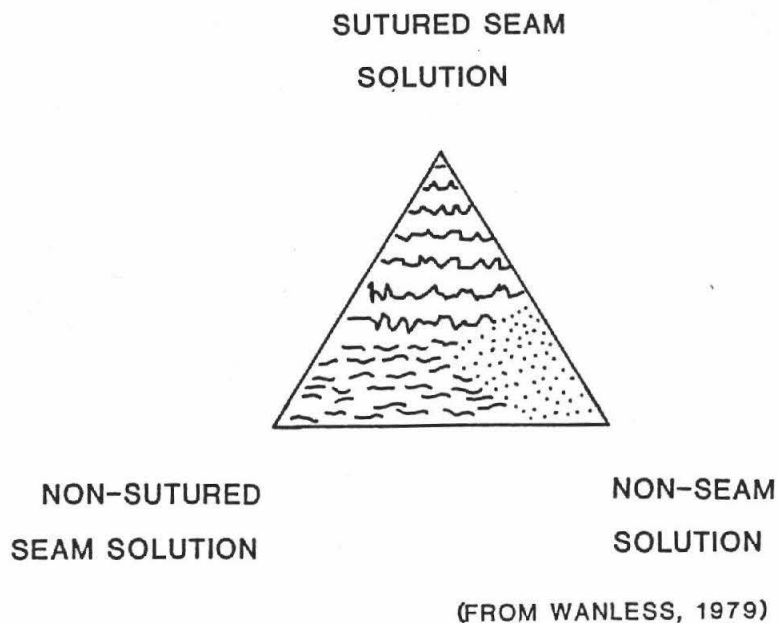


Figure 6: Diagrammatic representation of the genetically based classification of pressure-solution seams of Wanless (1979).

insoluble platy material. Because the rock is structurally resistant, the surrounding rock is relatively unresponsive to pressure solution.

The second type of pressure-solution response delineated by Wanless (1979) is the non-sutured seam solution surface or microstylolite. This morphology tends to form in limestone units that contain a significant amount of platy insoluble material. This type of seam often forms thin, anastomosing, wispy seams, that occur in swarms. Wanless proposed two reasons why microstylolites form in anastomosing swarms: (1) the accumulation of the platy insoluble material along the early form of the seam chokes off the migrating intrastratal solution and prevents further solution along that surface, and (2) the accumulation of platy insoluble material along the seam acts as a glide surface along which stress can be relieved. The relief of stress along the principle stress directions inhibits the formation or growth of the sutured form of pressure response.

The third type of pressure-solution response, the non-seam solution-dolomitization, occurs in limestone units that have little or no internal structural resistance. This type of pressure-solution response, unlike the previous two types, does not occur along a solution plane, but rather is pervasive throughout a unit. All three of Wanless's (1979) pressure-solution responses can generate a

physical and chemical environment that acts as the host for dolomite growth due to pressure solution. Among the three types, however, the sutured seam response is the least likely to be associated with pressure solution related dolomitization.

Although the classification of Wanless (1979) is widely used, there are drawbacks. All of his categories have very firm genetic implications. This makes his classification less useful as an initial descriptive tool, because it is difficult to separate his categories from his genetic interpretations.

Buxton and Sibley (1981) argue that the cementation history of a limestone is the most important parameter in deciding what type of pressure solution will occur. In their paper, they classify pressure solution into three categories: stylolites, solution seams, and fitted fabrics (Fig. 7).

Stylolites are defined as boundaries between units with a serrated form that often has insoluble material along it (Buxton and Sibley, 1981, p.20). Within the stylolite classification they make two subdivisions: Type 1A and 1B stylolites. Both of these subdivisions are serrated, but Type 1B has a higher frequency and a lower amplitude than Type 1A. Solution seams are undulating, smooth boundaries with accumulations of insoluble material similar to Type 1 stylolites, but lack a serrate habit

Pressure-Solution Seam Classification

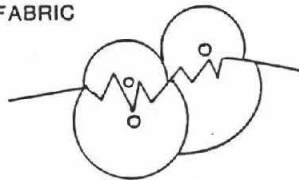
STYLOLITES



SOLUTION SEAMS



FITTED FABRIC



(After Buxton & Sibley, 1981)

Figure 7: Diagram of the pressure-solution seam classification of Buxton and Sibley (1981) based on the morphology of the seams.

(Buxton and Sibley, 1981, p.20). Fitted fabric is formed by intergranular pressure solution that occurs pervasively throughout a rock. Fitted fabric can be classified into two categories, limited fitted fabric, and unlimited fitted fabric. The difference between the two subdivisions is that limited fitted fabric occurs only in a zone a few grains thick that is surrounded by rock showing no fitted fabric textural characteristics. In contrast, unlimited fitted fabric is not restricted to a vertical dimension of a few grains in thickness, but can be of any thickness

(Buxton and Sibley, 1981, p.20). Buxton and Sibley's (1981) categorization for pressure solution is based mostly upon morphology, making only weak genetic inferences. This is in contrast to Logan and Semeniuk's (1976) strictly morphological classification and Wanless's (1979) classification that makes strong genetic inferences, and, as such, the classification plan of Buxton and Sibley (1981), is a more suitable approach to the description of pressure-solution responses.

Besides their pressure-solution feature classification, Buxton and Sibley (1981) derived two very important concepts from the analysis of their data: 1) the cementation history of the rock, and not its texture, dictates the style of pressure solution that is to occur, and 2) carbonate put into solution is not re-precipitated locally in pressure shadows, but is carried away from the area of active pressure solution. This contrasts with earlier suggestions that the solutes of pressure solution are mainly precipitated locally as cements (Wanless, 1979).

Reactate Dolomite

The term reactate is defined as a mineral that forms on a pressure-solution seam. This term does not have any mineralogic implications, but the most common reactate

mineral reported in the literature is dolomite (Logan and Semeniuk, 1976, Wanless, 1979, Mattes and Mountjoy, 1980, Jorgensen, 1983).

Although dolomite is often found, rarely in the literature is a satisfactory explanation offered. Logan and Semeniuk (1976) and Wanless (1979) do little more than mention the presence of dolomite and indicate that clays play a role in the formation of reactate dolomite by acting as sources of magnesium ions. Mattes and Mountjoy (1980) discuss burial dolomites, of which I consider reactates to be a subset, in some detail, and many of their ideas contributed significantly to the ideas presented in this report. Mattes and Mountjoy (1980) state that deep burial conditions are ideal for dolomite growth. The increased temperature of burial speeds up dolomite reaction rates and makes Mg^{++} available for dolomite formation. They also explain that the chemical environment and the reaction rates of the deep subsurface are favorable for the growth of burial dolomites.

One of the difficulties in explaining burial dolomite formation has been to provide enough Mg^{++} to grow a dolomite crystal. Mattes and Mountjoy (1980) were among the first to seriously consider the source of the Mg^{++} ions. They suggest two principle sources, connate water and clay mineral transformations. Kahle (1965) had earlier suggested that clay mineral transformations in the

subsurface could provide Mg^{++} to formation water systems. McHargue and Price (1982) once again use clay mineral transformations, specifically the smectite to illite conversion, as a source of Mg^{++} .

Methods

The Birdbear Formation (Devonian) of the Williston Basin was chosen as the subject of this study for two important reasons. First, reconnaissance showed the Birdbear to have abundant pressure-solution features. Second, the Birdbear was well represented in drill cores from the Williston Basin, so that there would be an adequate number of samples to work with. The drill cores used for the study were chosen to produce a bimodal spacing between cores. A set of closely spaced cores were chosen so that local variations might be noted. A second set of widely scattered wells was chosen to allow for the observation of changes that might manifest themselves only on a large scale.

Once the cores were chosen, the next step was to make macroscopic descriptions of the core in order to become acquainted with the lithologies of the Birdbear Formation. During the course of the description of the core, any gross variations in pressure solution style as a function of depth or lithology was also noted. In the early portion of

this work it became evident that the pressure-solution features were too small for macroscopic observation to reveal any important information. The last step in working with the core was the sampling of the core for thin section billets.

The sampling of the cores for thin sections was done subjectively; samples were chosen that contained representative examples of the types of pressure-solution features wanted. The only specific sampling plan was to obtain samples from each distinct lithology within a given core. In all, 11 cores were described and 218 billets were cut for thin section preparation.

After the thin sections were made from the billets, the thin sections were polished using descending sizes of polishing grit, with the final polishing completed with 0.05 micrometre aluminum oxide powder. The thin sections were polished to improve the resolution of fine features in the samples during light microscope inspection and to prepare the samples for scanning electron microscope (SEM) analysis. The final step in thin section preparation was to stain each thin section for calcite using alizarine red with a dilute hydrochloric acid base.

The characterization of the thin sections involved observation using a petrographic microscope, a microfiche reader and SEM and electron probe microanalysis (EPMA). The petrographic microscope and microfiche reader were used

to perform the general thin section descriptions and to take measurements of pressure-solution seam sizes. The SEM was used to gain a better description of the contents of the pressure solution seam and detailed spatial relations of those components. Qualitative EPMA was used to identify minerals that could not be positively identified using light microscope techniques.

The qualitative and quantitative chemical analyses of the phases in the thin sections were done using a JEOL 35C Scanning Electron Microscope with an energy dispersive spectrometer. The electron beam source was a tungsten filament. For the qualitative work, a 15kV accelerating voltage and a 1000 picoamp (pA) beam was used.

Quantitative analyses were done with an accelerating voltage set at 20kV and a 2000 pA beam with live count times of 100 seconds. These operating parameters were chosen from several combinations because they produced the best results for the elements of interest. Best results were determined by comparing lower limit of determination values measured and calculated from standard reference materials.

The lower limit of determination was chosen as three times the lower limit of detection as given by Jenkins (1974). The spectra from the sample were reduced to percent oxide values by a Bence-Albee reduction program (Bence and Albee, 1968, Goldstein, et al., 1984).

Pressure-Solution Terminology

In response to the numerous methods of classifying pressure-solution responses detailed above, I now propose a loose system for classifying pressure-solution responses based on morphology. This system combines the useful parts of Logan and Semeniuk (1976) and Buxton and Sibley (1981). In this report, the term "amplitude" refers to the vertical distance from the apex of a peak to the apex of an adjacent valley and the "wavelength" is the lateral distance between two adjacent peaks or valleys (Fig. 8).

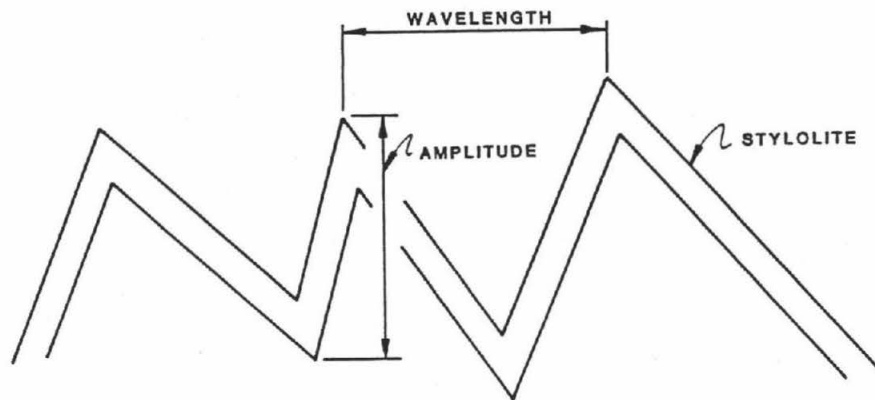
Definition of Amplitude
and Wavelength

Figure 8: The definition of amplitude and wavelength of stylolites. The amplitude is the vertical distance from apex to apex. The wavelength is the lateral distance from peak to peak.

The terminology applied to pressure-solution seams should be based solely on morphology of the feature and should make no genetic implications. In this way the term is of greater use as an adjective because it only describes, and allows the individual worker to determine genetic interpretations.

The overly detailed categories of Logan and Semeniuk (1976) combine well with Buxton and Sibley's (1981) more general classification system. In much of my original descriptions, the seams were put into the most specific categories possible. Later, after analysis of the descriptions and the data, a more general scheme was adopted.

Within the framework shown in Figures 4 and 7, all of the pressure-solution features seen in the samples studied fit into two broad categories: stylolites and solution seams. Within the stylolite category, three divisions were determined: columnar; peaked, high amplitude; and peaked, low amplitude (Logan and Semeniuk, 1976). All other seam morphologies fit into the solution seam category. Common members of this category were clay seams, and the "wavy" or "wispy" seams that Wanless (1979) calls microstylolites. In defining these categories, it was my intention to avoid implying any genetic associations during descriptions.

PRESSURE-SOLUTION RESPONSE

Introduction

In this study of pressure-solution response, the variables of interest are the wavelength and amplitude of the pressure-solution seam and the parameters that influence their size and morphology. This study focuses on the influence that depth and the texture of the host rock exert on the overall pattern of pressure-solution response.

Description of Pressure-Solution Response

Pressure solution occurred throughout the carbonate section of the Birdbear Formation. Both of the pressure-solution types, stylolites and solution seams, were found in all of the carbonate rocks, although there was a texture dependent preference which will be discussed in later sections of this report. The stylolites were of columnar and peaked morphologies (Fig. 9). The columnar form was often due to an allochem, usually a bioclast, occurring at the apex of a seam, causing the columnar shape (Fig. 10). Solution seams occurred in a variety of shapes as both tight and loose swarms as well as clay seams (Fig. 11). An unusual combination of solution seams and stylolites occurred in several places in the studied section. In

Figure 9 (top): Photomicrograph of a stylolite with both peaked and columnar forms. Field of view is 2 millimetres.

Figure 10 (bottom): A photomicrograph showing an iden in a typical position (arrow) displacing a pressure- solution seam. Field of view is 2 millimetres.

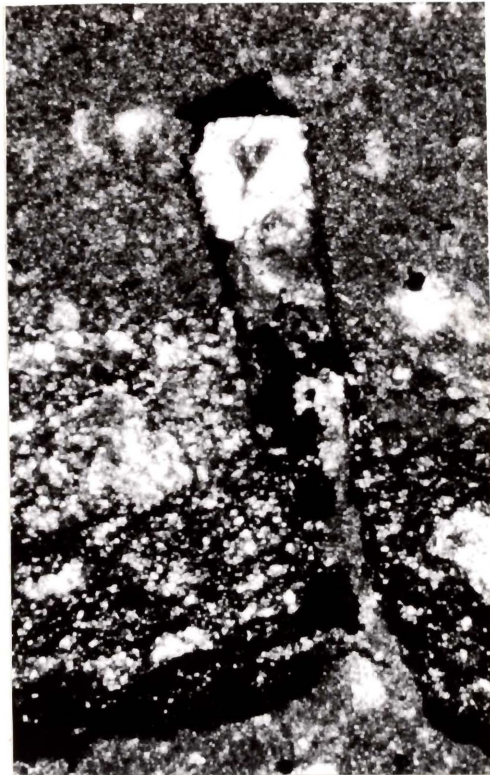
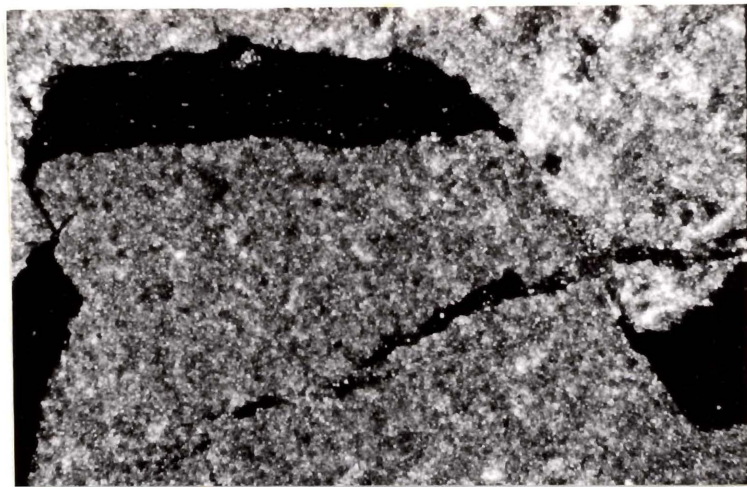
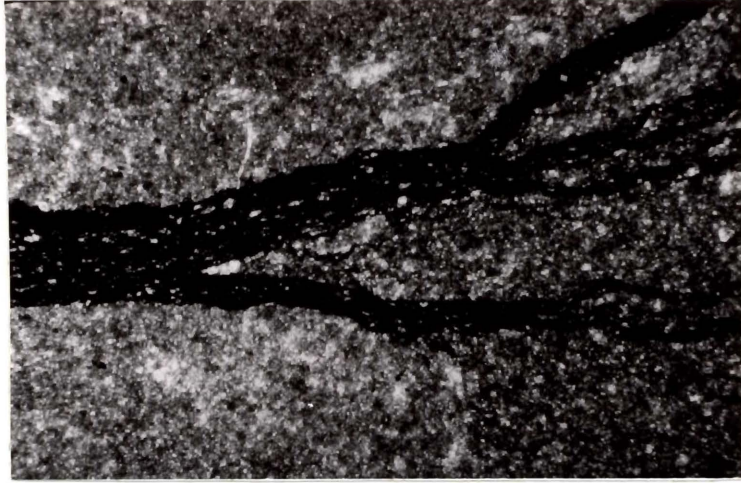


Figure 11 (top): A photomicrograph of a solution seam. Field of view is 2 millimetres.

Figure 12 (bottom): A photomicrograph of the unusual occurrence of a stylolite overprinting a solution seam. Field of view is 2 millimetres.



these instances, a swarm of solution seams was overprinted by a stylolite, typically columnar in form (Fig. 12).

With regard to the allochemical components of the rock, pressure-solution reactions occurred in three forms: inter-idenic, intra-idenic and circum-idenic. The inter-idenic seams "zig-zag" through the matrix between idens. The intra-idenic seams formed either exclusively within an iden or passed through an iden. The circum-idenic seams wave and "zig-zag" around the idens, surrounding them. The inter-iden seams were the most abundant, with both stylolites and solution seams present. The intra-idenic seams were almost always stylolites and occurred only rarely. The circum-idenic seams were most often solution seams, but occasional stylolites of this form were observed.

A definite set of parameters controlling whether a pressure-solution seam was inter-idenic, intra-idenic, or circum-idenic was not observed. It seemed to be a matter of chance, with the intra-particle seams being the least abundant, and therefore perhaps requiring special circumstances for formation.

The location of pressure-solution seams followed no regular pattern, but, as reported by Wanless (1979) and Buxton and Sibley (1981), pressure solution tends to occur more commonly at sites of inhomogeneity within a rock. Inhomogeneous sites can be considered on two scales, large

and small. Large scale inhomogeneities, the type most often cited (Wanless, 1979, Buxton and Sibley, 1980), usually occur at the contact between lithologic types. Small scale inhomogeneities, which were much more abundant within the study section, occur at allochem-orthochem boundaries. A typical allochem-orthochem contact would be between bioclasts and the surrounding micritic matrix (Fig. 13). Seams that were initiated at allochem-orthochem boundaries also varied in size. The smaller sizes sometimes extended laterally only a fraction of a millimetre, while larger sizes often extended the width of the thin section or core (3 to 10 centimeters).

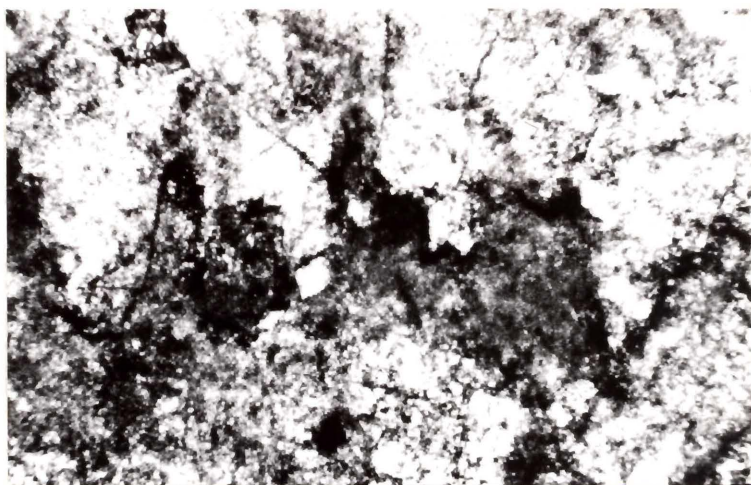


Figure 13: A photomicrograph showing a seam occurring at the textural inhomogeneity of the allochem-orthochem boundary. The allochem (upper portion of photo) is a stromatopore. Field of view is 2 millimetres.

Procedure and Data

Since pressure solution is in part a function of the amount of pressure exerted on the rock, it follows that amplitude and wavelength, elements of pressure-solution response, could show sensitivity to varying pressures. In the studied section, variations of pressure were due to change in depth within individual wells or to the overall change in depth of the study section within the Williston Basin.

To investigate the affect of depth, two relations were studied: (1) the relation of wavelength and amplitude sizes as a function of depth within individual wells and (2) the relation of wavelength and amplitude between wells.

In addition to the variation of pressure-solution response to pressure, there have been suggestions in previous studies that there is a correlation between the style of pressure-solution response and the texture and lithology of the host rock (Wanless, 1979). Wanless (1979) suggested that sutured seam responses occur in clean, structurally resistant limestones; that non-sutured seam responses occur in structurally resistant limestones that contain significant amounts of clay and silt; and that non-seam solution occurs in limestones that have low structural resistance and that contain little or no clay and silt. This study investigates the style of pressure-solution

response and the limestone texture and lithology in which it occurs. Also, if the textural type of the rock was an important influence in determining the style of pressure-solution response, it is possible that the textural type might also influence the relation between the amplitude and wavelength.

To investigate this possible relation, the shapes of pressure-solution seams were measured and the host texture or lithology noted. The pressure-solution features measured in this study were chosen in the following manner. A line was drawn parallel to the horizontal orientation of each thin section with the thin section correctly oriented in the up/down position. Using an optical microscope, the line was traversed, beginning on the right side, until a peak or valley of a pressure-solution feature was found that came closest to the line. In a case when two apices were equi-distant from the line, the apex first encountered was chosen. The wavelengths and amplitudes were then measured from the chosen apex. Three wavelengths and three amplitudes were measured moving to the right from the initial measuring point. If three wavelengths were not available, the seam was disqualified and the next nearest seam was chosen and the procedure repeated. Once the measurements were taken, the values for each measurement were averaged and noted.

The above procedure was developed and used to introduce randomness in the choice of the seams to be measured. This had to be done because the initial sampling of the core was done in a non-random manner that could possibly influence the results.

To investigate the variation of solution-seam morphology between textural types, the samples were divided into the following lithologic and textural classes: packstone, wackestone, mudstone, dolomitic-anhydrite, and dolostone. Within each of these lithologic and textural classes, the number of each of the pressure-solution response types was calculated (Table 1).

SIZE PARAMETERS FOR STYLOLITES

TABLE 1 The average magnitude in millimeters for the three parameters. Each was calculated separately for the wackestones, packstones, mudstones, dolostones and the dolomitic-anhydrite.

LITHOLOGY	AVE AMP (mm)	AVE WAV (mm)	AVE THICK (mm)	No.
WACKESTONE	0.35	0.54	0.06	53
PACKSTONE	0.37	0.57	0.03	27
MUDSTONE	0.37	0.78	0.14	11
DOLOMITE	0.21	0.67	0.06	4
DOLOMITIC-ANHYDRITE	0.75	1.67	0.11	6

Discussion

The Influence of Depth on Pressure-Solution Response

Within individual wells, there was no apparent relation between the depth and the amplitude or wavelength of the pressure-solution features. The apparent lack of influence of depth within individual wells may be because of the relatively small change in depth within a well caused by the thinness of the Birdbear Formation in the study area.

In contrast, a trend of increasing amplitude and wavelength with increasing depth is shown by graphing amplitude versus depth and wavelength versus depth (Figs. 14 and 15). There are some anomalies within this general trend. Some relatively deeper wells have stylolites with smaller amplitudes and wavelengths than shallower wells. The trend is more clearly seen if wells are viewed as either shallow, 4000 to 6000 feet, or deep, greater than 6000 feet. Using this distinction, the deep wells clearly have higher amplitudes and wavelengths than the shallow wells (Figs. 14 and 15).

Because the amplitude is an indicator of the minimum amount of rock material lost to pressure solution, it may be considered the most significant of the variables (Bathurst, 1975; Buxton and Sibley, 1981). It follows

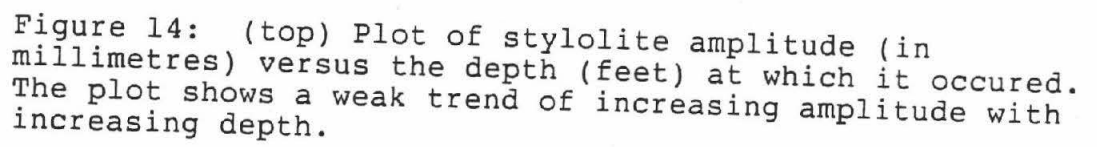


Figure 14: (top) Plot of stylolite amplitude (in millimetres) versus the depth (feet) at which it occurred. The plot shows a weak trend of increasing amplitude with increasing depth.

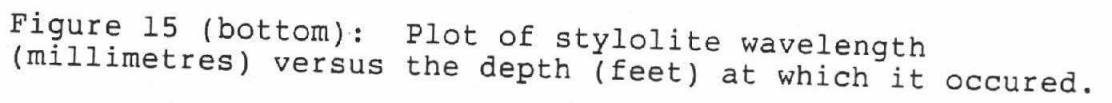
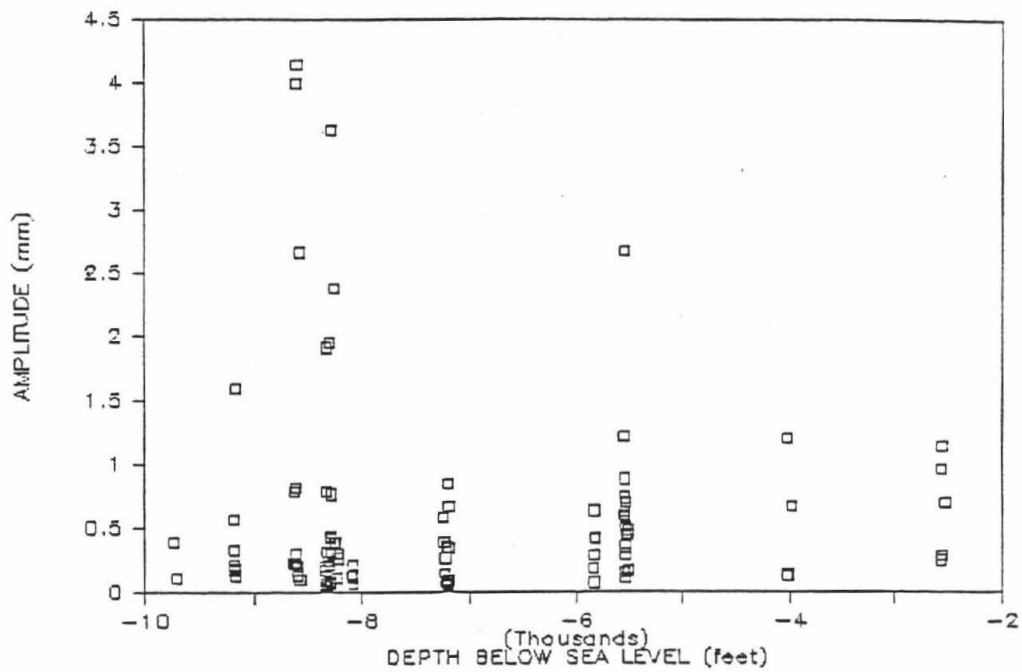
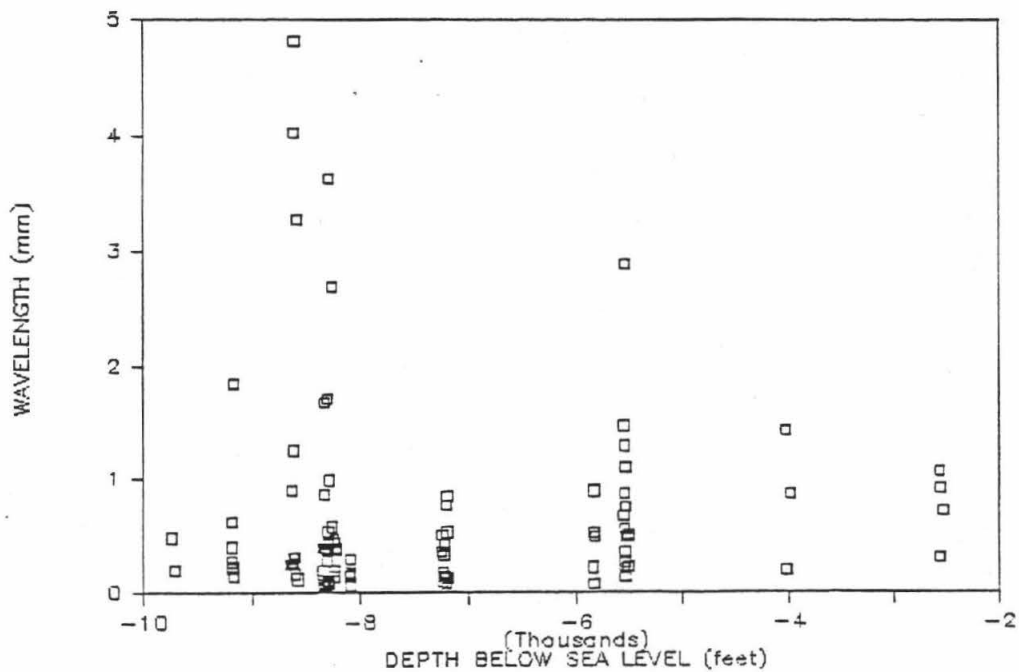


Figure 15 (bottom): Plot of stylolite wavelength (millimetres) versus the depth (feet) at which it occurred.

THE RELATION OF AMPLITUDE TO DEPTH



THE RELATION OF WAVELENGTH TO DEPTH



that pressure-solution seams at greater depths may be expected to have greater amplitudes because they are under greater stress for a longer time, and therefore more material may have been lost into solution. The trend of increasing amplitude with increasing depth (Fig. 14) is somewhat rough because the amount of rock material lost to pressure solution is not only a function of the amount of vertical pressure, but is also a function of the texture and cementation history of the rock.

Host Rock Influence on Pressure-Solution Response

Four of the five textural/lithologic classes defined earlier had solution seams as the most abundant type of pressure-solution response (Table 2). The one exception was in the packstone category, where the number of peaked, low-amplitude stylolites was more abundant than in the other categories.

This result is reasonable when it is recalled that packstones most closely approach grainstones in regard to textures, and grainstones are a textural type where stylolites, rather than solution seams, would be expected to be more abundant (Buxton and Sibley, 1981).

The magnitude of the wavelengths and amplitudes for pressure-solution features in the packstones and wackestones were very similar, with magnitudes in the

wackestones averaging slightly less at each measurement site. The dolomitic-anhydrite lithology had the largest amplitudes (average of 0.75mm) and wavelengths (average of 1.67mm) of the designated lithologic or textural types.

These results are to be expected since the crystalline nature of the dolomitic-anhydrites makes them similar to grainstones which are structurally resistant and tend to have large amplitudes (Wanless, 1979). The large wavelengths result from the direct relation between wavelength and amplitude where they increase and decrease in size proportionally (Fig. 16).

THE NUMBER AND TYPE OF PRESSURE-SOLUTION SEAM FOR EACH LITHOLOGY PRESENT

Table 2 The percentage and number of each stylolite type in each texture type, i.e. packstone (PACK), wackestone (WACK), mudstone (MUD), dolostone (DOLST), and dolomitic-anhydrite (DA) was calculated.

	COLUMNAR (%)	PEAKED, HI (%)	PEAKED LO (%)	OTHER (%)
PACK	14.81	7.41	48.15	29.63
WACK	11.32	12.50	32.08	49.06
MUD	0.0	18.18	18.18	63.64
DA	16.67	0.0	33.33	50.00
DOLST	0.0	0.0	25.00	75.00
TOTAL	10.89	7.92	34.65	46.55

According to Wanless (1979) and Buxton and Sibley (1981), mudstones and muddy rocks in general should respond to pressure solution in a non-structural manner, ergo forming solution seams rather than stylolites. It was, therefore, an unexpected result of this study that pressure-solution response in the mudstones were often stylolites and had amplitudes and wavelengths of the largest magnitude. The anomalously high values for the

RELATION OF WAVELENGTH AND AMPLITUDE

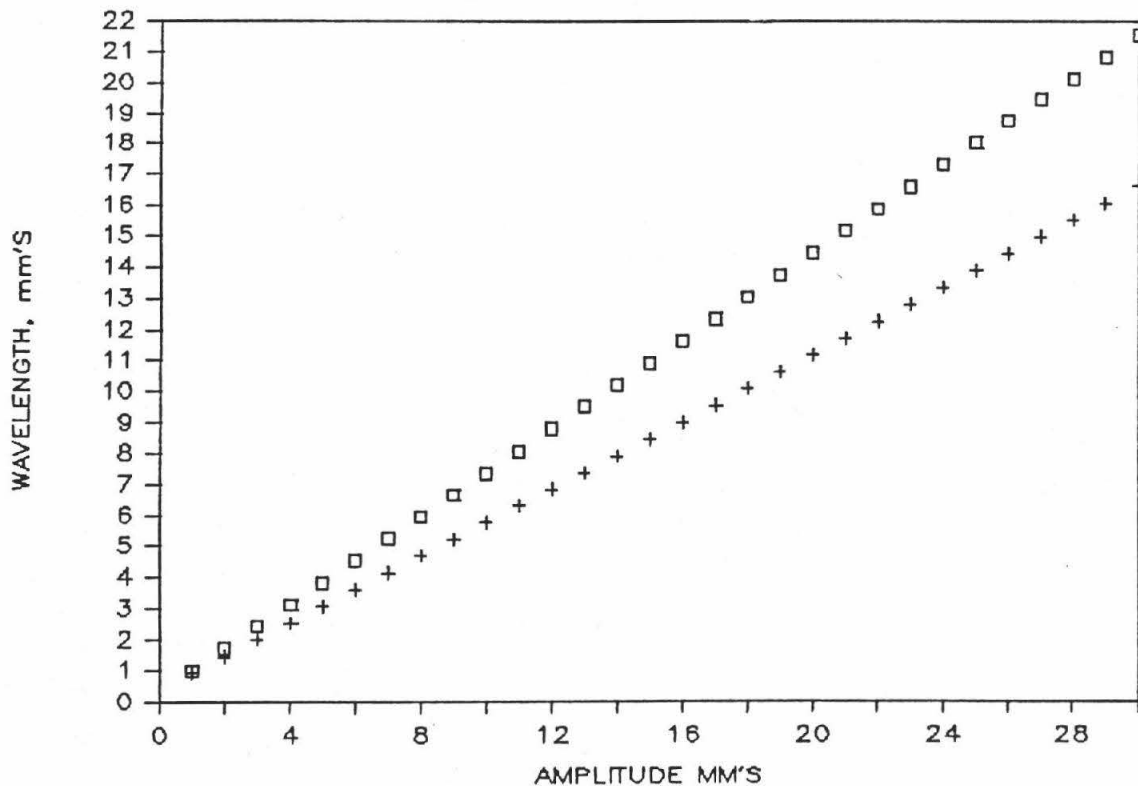


Figure 16: A best fit plot of wavelength versus amplitude for packstones (boxes) and wackestones (pluses).

amplitudes and wavelengths in the mudstones can be explained in two ways. One explanation is that mudstones with high amplitudes and wavelengths were cemented early, making them structurally resistant units which, according to Wanless (1979), should produce stylolites. The second explanation is that cement was present in local patches, creating a mudstone with locally well-cemented bodies, or idens that were resistant to pressure solution (Logan and Semeniuk, 1976). Then in the manner of idens, they could displace the zone of pressure solution, creating the stylolites with high amplitudes.

A plot of amplitudes versus wavelengths from the two most abundant textural types (Fig. 16), wackestones and packstones, shows that the two textural types have similar y-intercepts, but that the slope of the packstone plot is less steep. This indicates that the wavelength of the pressure-solution feature may be influenced, at least in part, by the presence of allochems, which act to inhibit vertical displacement. If allochems do act as inhibitors of vertical displacement, then the concept that the structurally resistant grainstones should have the largest stylolites (Wanless, 1979) should be dismissed.

MINERALOGIC CHANGES DUE TO PRESSURE SOLUTION

Introduction

Among the several physico-chemical processes that occur along or near a pressure-solution seam, the formation of minerals by precipitation and alteration along the solute-rock interface is among the most evident. The term given to these minerals is "reactate" (Logan and Semeniuk, 1976). The most commonly reported reactate mineral is dolomite (Logan and Semeniuk, 1976; Wanless, 1979; Buxton and Sibley, 1981), but calcite, mica, and chlorite have also been observed as reactate minerals (Logan and Semeniuk, 1976). The following discussion will detail analyses of selected dolomite rhombs thought to be reactate dolomite, and will propose several steps by which reactate dolomite formed in the study section.

Reactate Dolomites

A potential problem exists in distinguishing reactate dolomites from some other types of authigenic dolomite, i.e. point-source burial dolomite, or isolated eogenetic dolomites. The subhedral to euhedral, dirty-looking dolomite rhombs can easily be mistaken for other types of dolomite with similar shape that form earlier and become

trapped in the pressure-solution seam. Fortunately, reactate dolomite can be easily distinguished from most other dolomite that occurs in the study section. The non-reactate dolomites either have the wrong texture, or occur in associations that make them easy to distinguish from reactate dolomite.

Mattes and Mountjoy (1980) and McHargue and Price (1982) describe a type of dolomite, diffuse microcrystalline dolomite, that is difficult to distinguish from reactate dolomite. This dolomite type occurs as diffuse, micrometre size, clear, euhedral to anhedral rhombs that are found floating in micritic matrices. Often this diffuse type of dolomite becomes lodged on a pressure-solution seam as a stylocumulate. When this happens, it is very difficult to distinguish from reactate dolomite. The major difference between the two is that reactate dolomite is usually larger, more inclusion rich, and typically more abundant. The best way to distinguish reactate dolomite from diffuse, micrometre-sized dolomite is to peruse the areas adjacent to the pressure-solution seam and determine the amount of diffuse dolomite rhombs in the micritic matrix. If the adjacent matrix is free or almost free of the diffuse dolomite, then the dolomite that does occur on the seam can be categorized as reactate dolomite.

Description

The dolomite that was classified as a reactate mineral was typically euhedral to subhedral, with occasional anhedral forms, 50 to 100 micrometres on a side. The dolomite rhombs usually have a red-brown, dirty appearance with either poor extinction, non-extinction or areas of non-contiguous extinction (Figs. 17 and 18).

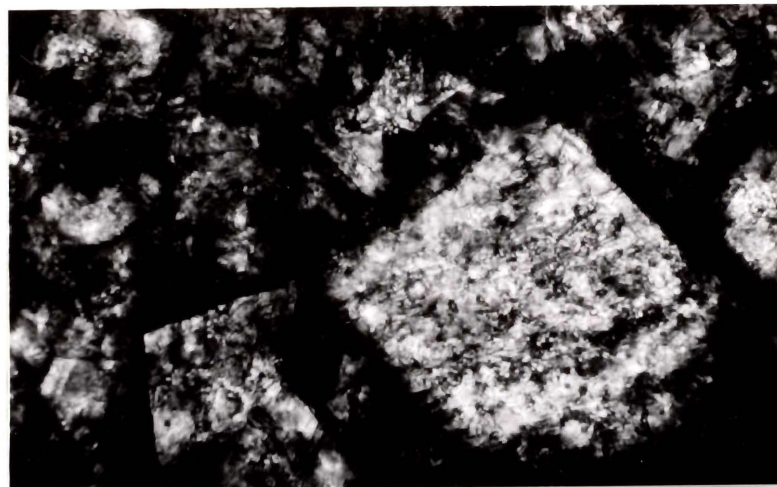
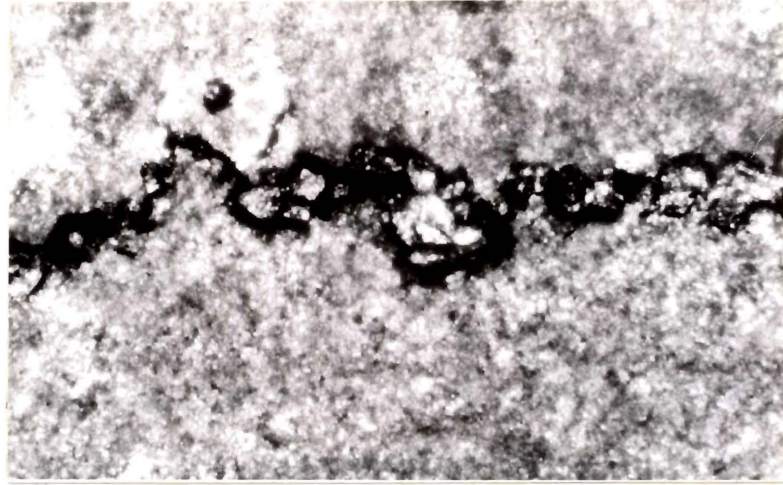
Reactate dolomite occurred in or against the seam it was related to. The type of pressure-solution feature and the thickness of the seam had no influence on the occurrence of reactate dolomite. Reactate dolomite rhombs often had dimensions larger than the thickness of the seam that they were associated with.

Electron microprobe analyses were obtained on twenty-eight selected reactate dolomite crystals to determine the general chemistry and the Mg^{++}/Ca^{++} ratio of the reactate dolomite. The settings for the SEM/EPMA were chosen specifically for the measurement of magnesium and calcium content.

The chemical results showed that the reactate dolomites analyzed were slightly calcium enriched and only occasionally contained cations besides calcium and magnesium. Other cations that were detected were iron, manganese and silicon, but usually only in amounts near the minimum determinable limits of the SEM/EPMA.

Figure 17 (top): Photomicrograph of reactate dolomite along a pressure-solution seam. View is approximately 2 millimetres across.

Figure 18 (bottom): Photomicrograph of reactate dolomite showing usual rhomb shape and inhomogeneous composition. Dolomite rhomb is approximately 0.15 millimetres across.



The Ca^{++} enrichment found was very slight, with $\text{Mg}^{++}/\text{Ca}^{++}=0.8035$. The very slight enrichment in calcium can have two sources, non-stoichiometry of the dolomite and artificial raising of the calcium ion by the presence of calcite inclusions. In the reactate dolomites in the studied rocks, the calcium enrichment is thought to be due not to non-stoichiometry, but rather to calcite inclusions. Regardless of whether the inclusions are of high or low magnesium-calcite, there would be enough "extra" calcium to cause the enrichment. This effect occurs because the interaction between the sample being analyzed, the dolomite rhomb, and the electron beam encloses a volume (approximately 4 micrometres) large enough to incorporate both the dolomite rhomb and its inclusions. This generates chemical data for the dolomite rhombs that is a combination of the dolomite and the impurities (Fig. 19). Thus, if the majority of the inclusions are calcite, the analyses will show an enrichment in calcium relative to the amounts expected from stoichiometric dolomite.

Discussion

This section will trace the origin of reactate dolomite from the original sedimentary environment to the production of a low magnesium-calcite rock with pressure-solution features and reactate dolomite. The discussion will illustrate how the chemical, kinetic, and spatial

organization of a pressure-solution seam is favorable to the growth of reactate dolomite.

Pre-dolomite Setting

The pressure-solution rich sections of the Birdbear Formation are composed almost entirely of micrite-rich textures, i.e. mudstones, wackestones or packstones. Therefore, any discussion of the nucleation and growth of reactate dolomites in the Birdbear Formation has to assume that these processes are taking place in a micrite-rich environment.

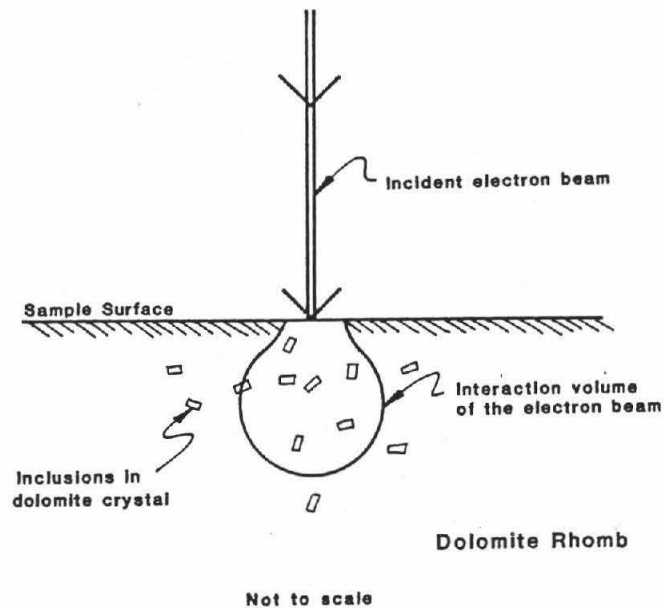


Figure 19: Schematic of the interaction volume of the electron beam of the scanning electron microscope and reactate dolomite. The size of the interaction volume causes the small, micrometre-size inclusions to be included in the dolomite analyses.

Eogenic Processes

Post-deposition and burial The description of the pre-dolomite environment given here is derived from Loeffler's (1982) environmental setting and is an eogenic, post depositional setting with the sediments still in contact with processes at the sediment-water interface. Initially, the sediment was a low permeability, high porosity, micritic carbonate containing interstitial fluids saturated with respect to CaCO_3 . With burial, several events occurred that are important to pressure solution. The two most important events are mechanical and chemical compaction. Significant changes in muddy sediments occur early in their burial history due to mechanical compaction. Shinn and Robbin (1983) demonstrated experimentally that mechanical compaction in carbonate muds begins early and does not require significant amounts of overburden. The first compaction event can cause a reduction of up to half of the original volume of a mass of sediment (Shinn and Robin, 1983). During volume reduction, the principle affect is a large reduction of the original porosity. This includes the flattening of root tubes, closure of fenestral pores, flattening of pellets, and closure of intergranular pores. Shinn and Robbin (1983) concluded that by simple mechanical compaction, porosity could be reduced to less than half of its original amount.

Another important occurrence during mechanical compaction is the concentration of organic material into thin wispy layers. These layers could very possibly be catalysts for the initiation of pressure solution during the chemical compaction stage (Shinn and Robbin, 1983).

Once mechanical compaction is nearly complete, chemical compaction, of which pressure solution is a subset, may begin. During both mechanical and chemical compaction, cementation of the sediments may take place and in some cases may be completed. In order for chemical compaction to occur, the sediments must be somewhat lithified, but cementation can continue during chemical compaction, further reducing initial porosity.

The major results of the two step compaction process are reduced porosity and permeability. The loss of porosity, due to the cementation of the sediments, and the loss of communication between surface fluids and processes and the rock unit due to permeability reduction defines the change from the eogenetic environment to the mesogenetic environment.

Continued burial allows two important and related steps in the diagenetic history of a sediment to begin: (1) the rock moves into a higher temperature and pressure regime and (2) pressure solution becomes a major diagenetic process.

Mesogenic Processes

Magnesium sources The move into higher pressure and temperature regimes and the initiation of extensive pressure solution is required to provide a source of Mg^{++} for the nucleation and growth of reactate dolomite. The increased pressure and temperature provides the Mg^{++} needed for dolomitization in three ways: (1) increased temperature causes the conversion of the clay mineral smectite to illite, releasing Mg^{++} (Kahle, 1965, Fasciolas and Powell, 1978, McHargue and Price, 1982), (2) magnesium present in the hydrated state is dehydrated, forming free Mg^{++} ions (Bathurst, 1975, Mattes and Mountjoy, 1980) and (3) pressure solution releases Mg^{++} that is present in the calcite of almost all limestones, even low Mg-calcite limestones (Logan and Semeniuk, 1976, Wanless, 1979, Buxton and Sibley, 1981). In addition, the elevated temperatures increase the rate of diffusion of Mg^{++} ions, making them more easily distributed within the fluid system.

The smectite to illite conversion process is important in the formation of reactate dolomites and is a well documented diagenetic process (Fasciolas and Powell, 1978) involving the exchange of exterior cations of the smectite with magnesium to produce illite, a diagenetically collapsed clay (Kahle, 1965, McHargue and Price, 1982). At near surface conditions, the ions that most readily replace

magnesium in the clay lattice are, in order of preference of exchange, calcium, potassium, and sodium. But under mesogenetic conditions, potassium is the most prolific replacement ion (Kahle, 1965, McHargue and Price, 1982). Therefore, under burial conditions the availability of the potassium ion controls the amount of Mg^{++} that can be released by the smectite to illite conversion. Fortunately, there are several sources of K^+ available in the diagenetic environment. The world ocean is a large storehouse of K^+ ions (Schmidt, 1973, Krauskopf, 1979) and two of the three sources of K^+ for the smectite to illite conversion are related to ocean sources: (1) K^+ adsorbed onto clays during contact with sea water shortly after burial, (2) dissolution of micas, and (3) potassium stored in organic matter that originated from lower life forms, i.e. algae (Krauskopf, 1979, McHargue and Price, 1982). Thus the K^+ ion needed to release Mg^{++} during the conversion of smectite to illite in the burial realm is readily available from each of these three sources, and shows the smectite to illite conversion to be a credible source for magnesium ions for dolomitization. This process was shown to be viable for the studied rocks using x-ray diffraction to show the presence of illite along pressure-solution seams.

The elevated temperature of the burial realm also increases Mg^{++} availability by catalyzing the dehydration of hydrated magnesium ions. Both Ca^{++} and Mg^{++} become

hydrated in natural systems, limiting their availability for use in diagenetic reactions. But the standard free energy of formation for Ca^{++} is more easily overcome, making it available at energies that leave Mg^{++} still attached to its water dipoles (Bathurst, 1975).

Increased temperatures also raise the rate of molecular speed, which directly increases the rate of diffusive movement of ions. Increased diffusion rates allow the ion species involved in reactate dolomite growth to be transported more readily within the fluid system (Berner, 1980). This increased mobility allows for limited amounts of Mg^{++} to be used in relatively widely spaced nucleation sites.

Increased pressure also influences Mg^{++} availability in the fluid system by releasing magnesium ions into the fluid system by pressure solution. Even low-magnesium carbonates contain enough Mg^{++} in their lattice structure to contribute significantly to the overall Mg^{++} content of the system (Buxton and Sibley, 1981, Mattes and Mountjoy, 1980).

Pressure solution Pressure solution is intimately involved in the formation of reactate dolomite as it provides part of the Mg^{++} needed for dolomite formation, much of the CO_3^- and Ca^{++} ions incorporated in the reactate dolomite, and a physical environment conducive to dolomite growth.

Besides being a source of ions, pressure solution also sets up an environment with a spatial organization that is ideal for the growth of reactate dolomite. This ideal set-up is composed of a three layer "sandwich" made-up of limestone, a boundary-layer of water and the concentrated insoluble material which is primarily clay (Fig. 20). It is this "boundary-layer sandwich" that sets up an environment that allows for the nucleation and growth of

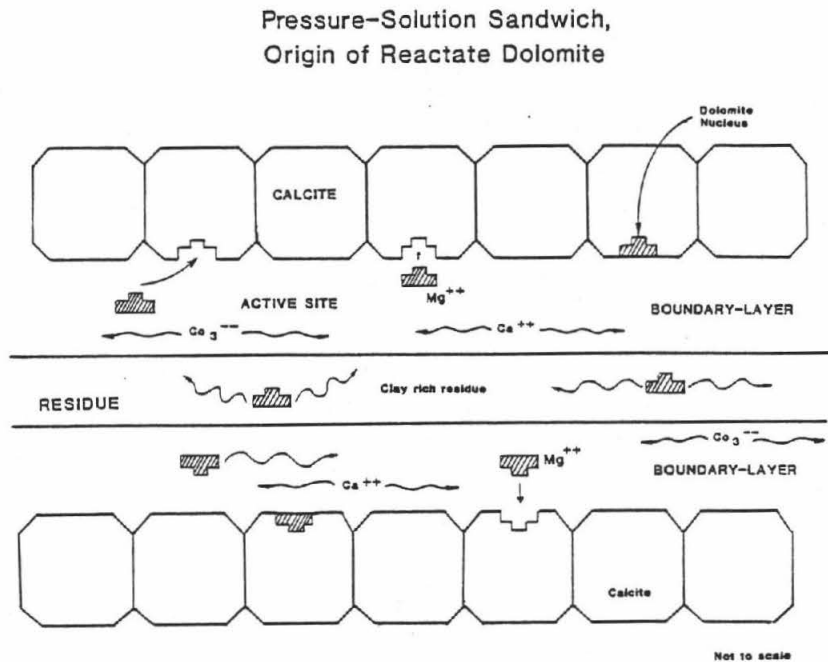


Figure 20: Schematic of the "pressure-solution sandwich" showing the three distinct parts: the central layer of insoluble residue, the boundary-layer of water and the host rock surrounding them. Also shown is the heterogeneous nucleation process that takes place along the host rock-boundary layer interface.

dolomite. Each layer of the "boundary-layer sandwich" contributes to the process. The limestone acts as a host for the growth of the reactate dolomite by possessing micrite crystals that are available as nucleation sites for crystal growth. The limestone is also a source for Ca^{++} , CO_3^{--} , and some of the Mg^{++} ions. Clays in the insoluble residue that forms most of the pressure-solution seam contribute most of the Mg^{++} ions needed for the growth of the reactate dolomite. The boundary-layer of water that is between the limestone and the insoluble material allows for the relatively rapid diffusion of the participating ions, particularly Mg^{++} , to the sites of reactate dolomite nucleation and growth.

Nucleation

If the physical set-up of the "boundary-layer sandwich" is established, and the ions needed for reactate dolomite formation, Ca^{++} , Mg^{++} and CO_3^{--} , are available, then the formation of the reactate dolomite can begin. The first step is nucleation, a process that occurs when maximum free energy in a system is attained and which involves the growth of sub-microscopic crystal embryos (Berner, 1980).

Two types of crystal nucleation are possible, homogeneous or heterogeneous (Berner, 1980). Homogeneous

nucleation involves the formation of the nucleus by the random collision of ions or atoms. Heterogeneous nucleation involves the nuclei forming on a substrate, sometimes referred to as a seed (Berner, 1980, Sibley and Gregg, 1987; Fig. 20). The very high number of suitable nucleating substrata in the sedimentary environment makes heterogeneous nucleation the most prolific nucleation mechanism (Berner, 1980, Sibley and Gregg, 1987). The nucleation seed can be thought of as a template with an atomic spacing similar to the newly forming crystal. In the formation of reactate dolomites, it is calcite that acts as the nucleation substrate (Sibley and Gregg, 1987). The setting in which nucleation is favored is one with high supersaturation with respect to dolomite and a substrate with many active sites, such as crystal-surface kinks (Berner, 1980, Sibley and Gregg, 1987).

Ionically, the vicinity of active pressure solution is ideal for dolomite nucleation because it is an area of high saturation with respect to dolomite. Ca^{++} , CO_3^{--} and some Mg^{++} are put into solution by pressure solution and additional Mg^{++} comes from the clays concentrated along the seam. In addition, the solution of the limestone along the pressure-solution seam causes etching of micrite crystal faces. This, combined with the high surface area to volume ratio of micrite, provides a relatively high number of active sites (Berner, 1980). Active sites are places on

the crystal surface that act as locations for the nucleation of the reactate dolomite. Once the nucleus crystal is formed, the next stage is crystal growth (Berner, 1980).

Crystal growth

There are two major factors that control crystal growth: (1) transport of reactants to the crystal growth site and (2) the rate of surface reaction (Berner, 1980, Given and Wilkinson, 1985, Sibley and Gregg, 1987). In some systems, either transport control or surface reaction control acts as the limiting factor in the growth rate of the new crystal. These factors may also act together to control growth rates (Berner, 1980). In the samples studied, both controlling mechanisms appear to have played an active role in the growth of reactant dolomites along pressure-solution seams.

The limited availability of Mg^{++} , one of the limiting factors in the nucleation of reactate dolomite, is also important in the growth rate of reactate dolomites. Given and Wilkinson (1985) have shown that the growth rate of abiotic carbonates is controlled by the availability of the least common ion. In the growth of reactate dolomites, Mg^{++} is the least common ion. Ca^{++} and CO_3^{--} are continuously produced in abundance along the pressure-

solution seam. But, sources of magnesium are rare and relatively local, depending on the concentration of clays, the successful conversion of smectite to illite, (the two principle sources) and the amount of Mg^{++} contained in limestone and connate waters.

Once Mg^{++} is made available, it must rely on diffusion to spread through inter-crystalline fluids to a site of nucleation (Fig. 20). The ions released into the fluid system have two principal directions in which they can migrate, horizontally, along the seam, or upward towards lower pressure. The pressure gradient prevents the ions from trying to migrate downward, towards higher pressures. In trying to migrate vertically, ions below the seam would have to pass through the relatively impermeable barrier of the pressure-solution seam, while ions above the seam would have to pass through the highly tortuous route between micrite grains or along fractures. The path along the pressure-solution seam is less tortuous and therefore relatively easier, a virtual ionic highway.

This "highway" is still only an intercrystalline boundary layer of water, but it should be significantly less tortuous than that encountered in intercrystalline boundary layers. In addition, the boundary layer may well be "thicker" than the intercrystalline pores (Fig. 20). Therefore, the boundary-layer of water in the "boundary-layer sandwich" should allow for easier migration of ions.

The relative ease with which ions move along the boundary-layer of water in the "boundary-layer sandwich" is important because the Mg^{++} is produced and introduced into solution at local, distinct sources by the processes discussed above. Once available, the Mg^{++} must travel by diffusion along the ionic "highway" to reach areas of crystal growth. It is because Mg^{++} availability is limited and migration of the ions is strictly due to diffusive movement, which is itself restrictive, that the growth rate of the reactate dolomite is controlled mainly by transport rate.

Gaines (1980) and Sibley and Gregg (1987) call upon surface controlled reaction rates as the controlling factor in the growth of mesogenetic dolomites, especially dolomite growing on low magnesium-calcite substrata (Gaines, 1982). It appears that both transport rate and surface reaction rate contribute to the pace of reactate dolomite crystal growth. Reactate dolomite growth rate is also controlled by surface reaction rate, which is a function of the rate of the chemical reaction(s) taking place during the growth of the new crystal.

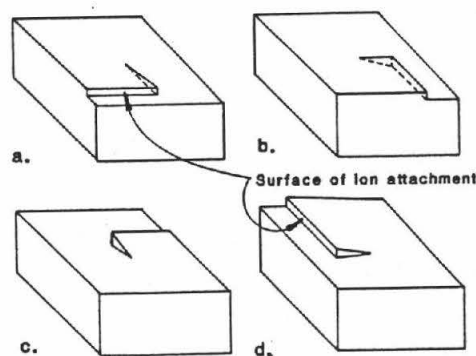
Because growth of the new crystal is influenced by surface reaction rates, crystal growth takes place by the addition of ions onto screw dislocation steps on the surface of the growing crystal. Screw dislocations, common

crystal defects (Fig. 21), provide sites of attachment for the ions involved in crystal growth (Berner, 1980).

The Resultant Reactate Dolomite

The processes and mechanisms involved in the formation and growth of the reactate dolomites have all had an influence on the physical make-up of the resultant reactate dolomite. The reactate dolomite crystals found during this study were euhedral, with numerous inclusions and varying patterns of extinction. The mostly euhedral shape of the reactate dolomites is probably due to their slow rate of growth and the solution-precipitation process that takes

Crystal Growth by Screw Dislocation



(from Berner, 1980)

Figure 21: The screw dislocation process of crystal growth. Growth of the new mineral takes place by the addition of ions onto the plane-surfaces of the screw dislocation.

place, allowing space for the crystal to grow (Sibley, 1982). The varying types of extinction patterns observed, non-extinction, normal extinction and non-contiguous areas of extinction, are dependent on the abundance of inclusions in the crystal structure. The more inclusions that are present, the less uniform the extinction properties of the reactate dolomite. If the number of inclusions varies locally within the rhomb, the rhomb will exhibit variations in its extinction pattern.

The Relation Between Pressure Solution and Neomorphism

A supposition at the beginning of this project was that there may exist a relation between pressure solution and neomorphism. To investigate this possibility, the occurrence of neomorphic calcite and its relation to pressure solution were studied.

Neomorphism is the polymorphic transformation of one mineral species to another or the recrystallization of a single mineral species (Bathurst, 1975). The neomorphic process of concern in this study is the recrystallization of micrite, less than 4 micrometres in diameter, to neomorphic spar greater than 5 micrometres in diameter.

Procedure and Data

To investigate the possibility of a relation between pressure solution and neomorphism, 217 petrographic thin sections were studied. For each thin section, the presence or absence of the following were noted: (1) dolomite, (2) neomorphic spar, (3) occurrence, whether the neomorphic spar was distinct from any dolomite present, or if they occurred in the same area of the thin section.

The dolomites of interest were divided into burial dolomites (Mattes and Mountjoy, 1980, McHargue and Price, 1982) and reactate dolomites. Individual dolomite rhombs that occurred away from the vicinity of a pressure-solution seam, in an area that showed no evidence of pervasive pressure-solution dolomitization (Wanless, 1979) were considered burial dolomite. Reactate dolomite in this report is defined as dolomite that occurs exclusively on or near a pressure-solution seam and that can be distinguished from stylocumulate.

From the original 217 petrographic thin sections available for study, 33 were not applicable to this portion of the study because of their lithology. The numerical breakdown of the data is contained in Table 3.

THE RELATION OF NEOMORPHISM AND PRESSURE SOLUTION

Table 3 The numerical data from the study of neomorphism's relation to pressure solution.

TOTAL NUMBER OF THIN SECTIONS	217	All petrographic thin sections available for study.
TOTAL APPLICABLE	184	From the original number of thin sections, 33 were not applicable to this study because of lithology.
TOTAL NEOMORPHIC THIN SECTIONS	94	The thin sections that contained neomorphic spar.
NEOMORPHIC THIN SECTIONS, NO DOLOMITE MIX	57	In these thin sections the neomorphic spar was in areas distinct from dolomite.
NEOMORPHIC THIN SECTION, DOLOMITE MIX	29	These thin sections had areas of mixed dolomite and neomorphic spar.
NEOMORPHISM ONLY	8	Thin sections that had areas of neomorphism, but contained no dolomite at all.

Description

The neomorphic calcite present in the study area is generally poorly developed and limited in extent. Most of the neomorphic calcite present has developed to a stage just beyond the upper limits of micrite. The crystal sizes of the neomorphic calcite are often so small that it is

difficult to distinguish from micrite. Only rarely had the neomorphic process progressed to the point where the resultant calcite crystals could be considered pseudospar (greater than 30 micrometres). In addition, the neomorphic calcite was never observed to be developed to the stage where it could be confused with calcite cement. Congruent with its poor size development, the neomorphic spar occurred only locally, in small patches or bands, rarely more than a few millimetres thick.

These small patches or bands, regardless of size, usually had very sharp boundaries with the non-neomorphosed portions of the rock. In addition, neomorphic calcite rarely occurred adjacent to a pressure-solution seam.

In most cases, the area adjacent to the pressure-solution seam was occupied by various amounts of dolomite. Independent of the amount of dolomite, dolomite and neomorphic calcite occurred together only half as many times as neomorphic calcite with no dolomite. In the instances where the dolomite rhombs and neomorphic calcite occurred together, the dolomite could be determined to have formed before the neomorphic calcite. These mixes were usually comprised of small, distinct, euhedral dolomite crystals surrounded by a thin blanket of micrite, which in turn were surrounded by neomorphic calcite. In many cases, a corner of a dolomite rhomb penetrated the micrite blanket and projected into the space occupied by the neomorphic

calcite. This placement suggests that the dolomite formed in micrite (calcite) before the onset of neomorphism, and then neomorphism caused replacement of the micrite around the dolomite rhomb. The only micrite left around the dolomite rhomb is a thin veneer shielded from the mechanisms of neomorphism by the rhomb.

Discussion

In the ideal situation, neomorphism takes place in three stages (Bathurst, 1975). The first stage is the nucleation stage. In this stage the most important process is the growth of stable crystals at the expense of other crystals. Sediment begins this stage with high porosity and permeability, yet cemented enough to be rigid (Bathurst, 1975). The second phase of neomorphism is the framework stage. During this stage of development, the neomorphic crystals begin to grow large enough to meet and form a rigid framework. The enlarging crystals cause a reduction in porosity and permeability, which in turn allows diffusion to be the major migration mechanism upon which further growth is dependent. The third stage of Bathurst's (1975) neomorphism model is the solution film stage. In this phase of development, the rock is pure calcite spar with only 1 percent to 2 percent porosity in solution films at inter-crystalline boundaries. Growth of

neomorphic calcite crystals continues by wet boundary migration, where crystals grow at the expense of their neighbors (Bathurst, 1975).

These stages of growth are reasonable, but they do not take into consideration the environment in which neomorphism is occurring. Further consideration must be given to the influence of two important parameters (1) the pressure and temperature regime, and (2) the presence of ions in the interstitial fluids that may affect the activities of recrystallization.

Affects of Temperature and Pressure on Neomorphism The use of logic suggests that the processes that cause the three stages of neomorphism are controlled by the same kinetics that govern other diagenetic processes. It might be useful to consider the neomorphic process as growth and solution by the exchange of ions between the inter-crystalline fluid and the solid crystalline phase.

The affects of temperature and pressure on neomorphic processes might be analogous to those discussed for pressure solution. Neomorphism could thus be a symptom of the same processes as pressure solution. Increased pressure and temperature cause dissolution of micrite grains, but if a pressure-solution seam does not form to distribute the newly freed ions away from the area, the inter-crystalline fluids become supersaturated, causing a

decrease in pressure solution. Then, if the supersaturated fluid re-precipitates as calcite, it would do so upon adjacent, larger crystals that act as seeds of growth.

Influence of Ions in the Intercrystalline Fluids The presence of certain ions in the intercrystalline fluids affects the neomorphic process by inhibiting both precipitation and dissolution. According to Folk (1974) if the inhibiting ions (in his case magnesium) were to be removed, then the neomorphic process could continue. The most prolific inhibiting ion in this case is magnesium, which occupies kink sites (active sites) on nucleating crystals, and prevents the active sites from participating in the solution-precipitation processes (Berner, 1980). Since the magnesium ion is present in the fluids associated with carbonate sediments, there must be some way to remove Mg^{++} , if neomorphism is to occur.

Folk (1974) suggests four ways in which Mg^{++} may be removed or its concentration decreased: (1) initial deposition in brackish water causes an initial low Mg^{++} content, (2) the soak-down of fresh water from fluvial sources into carbonate strata below diluting the Mg^{++} in the interstitial fluids, (3) Mg^{++} seized by interbedded or inter-carbonate crystal clay minerals and (4) flushing of the sediments by meteoric waters causing a decrease in Mg^{++} content. A fifth mechanism for the removal or lessening of

the Mg^{++} content in the system is proposed in this report. Magnesium is taken up during the nucleation and growth of mesogenetic dolomite. Of the first four mechanisms of magnesium removal, only number three (3), Mg^{++} being seized by interbedded or inter-carbonate crystal clay minerals, is possible for the rocks of this study. This study, however, illustrates that during mesogenetic diagenesis, clays are more likely to provide Mg^{++} than to remove it from interstitial fluids. Therefore, burial dolomite acting as a magnesium sink appears to be the primary means of decreasing the Mg^{++} content of intercrystalline fluids.

Mesogenetic Dolomite as a Magnesium Sink The two types of dolomite that are important as Mg^{++} sinks in the Birdbear Formation are point-source burial dolomite and reactate dolomite. Point-source burial dolomites are small, euhedral rhombs that occur disseminated in muddy rocks (McHargue and Price, 1982, Fig. 22). This type of dolomite forms from local sources of Mg^{++} derived from concentrations of clay particles. The clay particles provide magnesium to the system in several ways (See section on reactate dolomite, beginning on p.40). They adsorb magnesium during deposition and early diagenesis, to be released into the interstitial fluid in the mesogenetic environment. The clays also contribute magnesium to the interstitial fluid system by the conversion of smectite to

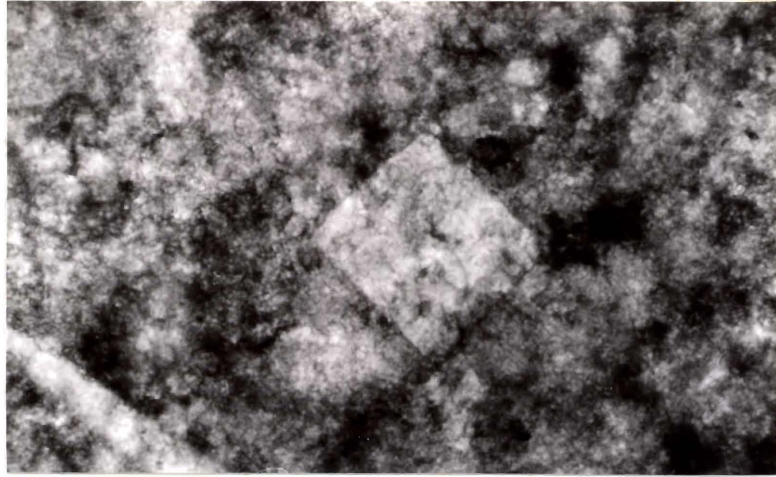


Figure 22: Photomicrograph of a point-source burial dolomite rhomb in micritic matrix. The field of view is 0.33 millimetres.

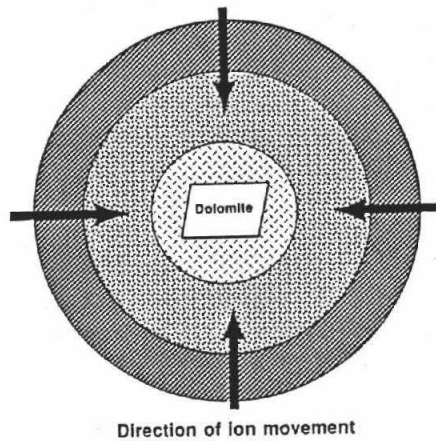
illite (McHargue and Price, 1982). Once the magnesium is released, nucleation and growth of point-source dolomites can proceed.

Whether the magnesium sink is reactate dolomite or point-source burial dolomite, the mechanism of depleting the Mg^{++} contained in the inter-crystalline pores is the same. Once dolomite formation begins, it causes a decrease in magnesium concentration in the vicinity of the growing rhomb (Berner, 1980). This causes a small-scale concentration gradient (Berner, 1980) and pulls Mg^{++} ions towards it to be used in the dolomite formation process (Fig. 23). The movement of the magnesium ions in this

system is by diffusion, so it is necessarily slow. Because the processes involved are controlled by diffusion transport rates, it is understandable that the effects can be very local.

From the data presented in Table 3 it can be seen that in the samples used for this study, only 8.5 percent of the thin sections that contained neomorphic spar did so without the presence of dolomite. In contrast, 95 percent of the thin sections that contained dolomite also contained neomorphic spar. From this data and the model proposed for removing Mg^{++} from the interstitial environment, I propose

Diagrammatic View of
Small-Scale Concentration Gradient
Developed During
Mesogenetic Dolomite Formation



Not to scale

Figure 23: Schematic of the small-scale concentration gradient that forms around mesogenetic dolomite crystals due to their growth in a muddy matrix. The concentration gradient causes the migration of the participating ions towards the growing dolomite crystals.

that mesogenetic dolomite can be an important component in the neomorphic process.

The second conclusion from this portion of the study is that neomorphic processes are not necessarily tied to pressure solution. Rather, pressure solution can help initiate neomorphism in its solution film stage by the removal of magnesium from the inter-crystalline fluid system during the formation of reactate dolomite. The nearest link that can be drawn between neomorphism and pressure solution is that the formation of point source burial dolomites, pressure solution and pressure solution dolomite can begin at similar temperatures and pressures and therefore at similar times in the history of a sample.

CONCLUSIONS

1. In regard to pressure-solution response, when classifying pressure-solution seams, two major morphology types can be used; solution seams and stylolites.
2. There is no evidence that amplitude or wavelength of pressure-solution features increases with depth within the fifteen to twenty metre thickness of the Birdbear Formation in individual wells.
3. There is a slight trend of increasing amplitude in wells from deeper portions of the basin. It is understood that this trend is minor and it could be an artifact of complicating factors such as cementation, chemistry or lithology.
4. Among the carbonate textures, pressure-solution features in packstones had the largest amplitudes, but from all lithologies, the dolomitic-anhydrite had stylolites with the largest amplitudes. The large values for dolomitic-anhydrite occur because of its structurally responsive nature, similar to that of a grainstone.

5. An unusual result is that mudstones show a higher percentage of peaked, high amplitude stylolites than do packstones and wackestones. This implies that parameters other than texture (as suggested by Wanless, 1979) play a role in determining the shape of a pressure-solution response.

6. The slope of the x-y relation between wavelength and amplitude is higher for wackestones than packstones. This may indicate that allochemical components in muddy carbonates act as inhibitors to vertical displacement of pressure-solution seams.

7. Clays concentrated along pressure-solution seams are a local source of Mg^{++} for dolomite formation.

8. The environment of the pressure-solution seam is ideal, physically and chemically, for the nucleation and growth of reactate dolomite.

9. Dolomite nucleates by heterogeneous nucleation on active sites on micrite crystals along pressure-solution seams.

10. Post nucleation growth occurs by the addition of ions onto screw dislocation steps on the crystal surface.

11. Crystal growth is controlled by transport rates and surface reaction rates.
12. Neomorphism and pressure solution are not intrinsically linked.
13. Formation of point-source burial dolomite and reactate dolomite helps to initiate neomorphism because both are active Mg^{++} sinks.
14. Neomorphism and pressure solution are related in that the timing of their formation may be close. The burial conditions that initiate pressure solution also initiate Mg^{++} up-take and neomorphism in these tight, muddy lithologies.
15. Mg^{++} is more likely to be added to interstitial fluids by clay mineral transformations than it is to be removed by adsorption on clays.

APPENDICES

APPENDICES
APPENDIX A
APPENDIX B
APPENDIX C
APPENDIX D
APPENDIX E
APPENDIX F
APPENDIX G
APPENDIX H
APPENDIX I
APPENDIX J
APPENDIX K
APPENDIX L
APPENDIX M
APPENDIX N
APPENDIX O
APPENDIX P
APPENDIX Q
APPENDIX R
APPENDIX S
APPENDIX T
APPENDIX U
APPENDIX V
APPENDIX W
APPENDIX X
APPENDIX Y
APPENDIX Z

APPENDIX A

DESCRIPTION OF THIN SECTIONS

Appendix A contains the data from the thin section descriptions. The data is divided into groups by wells, each labeled with a North Dakota Geological Survey Number. Column (1) is the depth from which the thin section was sampled; column (2) gives the orthochemical content of the thin section; column (3) gives the estimated allochemical content of the thin section; column (4) gives the estimated amount of dolomite contained in the thin section; column (5) gives the estimated amount of anhydrite in the thin section; and column (6) is an estimate of the amount of porosity in each thin section. In each column 2 through 6 the values are in percent; with the symbol "TR" representing "trace" for amounts less than one percent. The values are given as ranges because they are estimations.

Column (7) gives the lithology of the thin section in Dunham (1962) classification terms and where Dunham's classification is not applicable, mineralogical terms are given. For the Dunham (1962) terms, P = packstone, W = wackestone, M = mudstone. For the other lithologic terminology used, D = dolostone, and DA = dolomitic-anhydrite. In addition, the use of two lithologic symbols separated by a "\" signifies that the two lithologies are present in the thin section.

Column (8) gives the morphologic classification of the pressure-solution seams in the thin section. The symbol Roman numeral I represents a stylolite and a II represents a solution seam. Within the stylolite group (I) the letters A through D represent morphologic categories of stylolites; A = columnar, B = peaked, high amplitude, C = peaked, low amplitude, D = irregular. Within the solution seam category (II) the letters A through C represent the closeness of the solution seam swarm; A = loose swarm, B = tight swarm, C = clay seam. In this column, "NA" stands for "not applicable" and means that the thin section contained no pressure-solution seams.

THIN SECTION DESCRIPTIONS

1	2	3	4	5	6	7	8
NDGS# 286							
4105.0	25-30	5-10	45-50	0	0	W	ID, IIA
4102.5	40-45	25-30	15-20	1-3	TR	PW	ID, IIA
4098.0	35-40	20-25	20-25	3-5	0	P	IA, IIB
4097.0	15-45	20-40	3-40	TR-3	TR-1	P/WP	ID, IIA
4090.0	20-25	10-15	60-65	0	TR-1	W	IIB
4086.0	15-20	25-30	25-30	5-10	1-3	W	IIBC
4083.0	45-50	10-15	25-30	0	TR	W	IE, II BC
4082.0	20-25	10-15	45-50	3-5	TR	W	ID, IIB
4080.0	10-15	10-15	65-70	0	0	W	IIB
4079.0	10-15	15-20	50-55	3-5	TR-1	E	IB, ID
4070.0	25-30	25-30	15-20	10-15	0	WP	IC
4070.0	5-10	20-25	45-50	5-10	1-3	WP	ID, ICD, IIB
4069.0	5-10	5-10	65-70	3-5	TR-1	E	IC, ID
4065.7	15-20	1-3	30-35	20-25	3-5	W	ID
4065.0	10-15	20-25	20-25	45-50	TR-1	W	ID
4065.0	10-15	1-3	65-70	TR-1	TR-1	D	ID, IF
4064.0	30-35	5-10	35-40	0	0	W	ID
4058.0	TR	TR-1	65-70	0	0	D	IIB
4046.0	15-20	25-30	35-40	0	0	W	IIB
4040.0	1-5	5-10	10-15	70-75	0	DA	NA
4034.0	1-5	5-10	10-15	70-75	0	DA	NA
4025.0	1-5	5-10	10-15	70-75	0	DA	NA
4025.0	1-5	5-10	10-15	70-75	0	DA	NA
4022.0	45-50	10-15	30-35	TR	0	W	IC, IIB

NDGS# 4599

7508.0	55-60	30-35	TR	0	1-3	PW	NA
7506.0	35-40	40-45	1-3	0	1-3	PW	IAB, IIB
7503.0	25-30	25-30	5-10	TR-1	0	PW	IB, ICD, IIB
7502.5	20-25	30-35	1-3	TR	TR-1	P	IABD, IIB
7501.0	45-55	30-35	3-5	1-3	TR	PW	IC, IIB
7501.0	45-55	25-30	5-10	TR-1	TR-1	W	IAB, ID, IIB
7499.5	50-60	10-15	3-5	5-10	0	W	ICD, IIB
7499.5	40-50	25-30	0	5-10	1-3	P	IIB
7499.0	30-40	30-35	3-5	1-3	TR	W	IF, IIB
7499.0	30-40	45-50	3-5	TR	0	P	IID
7495.0	50-60	15-20	3-5	1-3	1-3	W	IC, ICD, IIB
7492.5	35-45	20-25	10-15	3-5	3-5	P	ICD, II BC
7490.6	35-45	30-35	5-10	1-3	TR-1	P	ICD, II BC
7490.0	40-50	20-25	10-15	3-5	3-5	PW	ID
7490.0	20-30	30-35	15-20	3-5	3-5	WP	IIB
7489.0	25-35	25-30	3-5	TR	1-3	W	ICD, IIC
7489.0	20-30	40-45	10-15	3-5	3-5	W	ID, IIB

THIN SECTION DESCRIPTIONS

1	2	3	4	5	6	7	8
7489.0	15-20	45-50	10-15	3-5	3-5	P	IB, IIC
7489.0	35-40	25-30	10-15	5-10	TR	W	ID, IIB
7488.0	35-45	15-20	20-25	5-10	TR-1	W	IIB, IIBC
7486.0	60-70	20-25	TR	3-5	1-3	W	IC
7486.0	35-45	25-30	0	15-20	3-5	W	IBC
7485.2	45-50	TR-1	10-15	15-20	15-20	M	IACD
7465.5	85-90	0	0	10-15	0	M	ICD
7455.5	90-95	0	0	5-10	0	M	IC

NDGS# 38

5557.0	60-65	5-10	15-20	1-3	0	D	NA
5556.0	0	0	85-90	1-3	1-3	D	IIB
5554.5	0	0	85-90	3-5	1-3	D	IIB
5553.0	0	0	85-90	3-5	1-3	D	ICD, IIB
5546.0	0	0	85-90	0	3-5	D	IIB
5546.0	0	TR	85-90	0	1-5	D	ID, IIB
5534.0	0	5-10	80-85	TR	TR-1	D	IIB
5530.0	0	0	90-95	TR	3-5	D	IIB
5528.0	TR	TR	85-90	TR	0	D	IIAB
5519.8	TR	0	30-35	55-60	0	D	NA
5517.0	0	0	80-85	5-10	1-3	D	NA
5514.0	TR	0	90-95	3-5	1-3	D	NA
5512.0	0	0	85-90	3-5	3-5	D	NA
5506.0	0	0	90-95	1-3	1-3	DA	IIB

NDGS# 2828

11420.0	60-65	15-20	3-5	1-3	TR	PW	ID, IIB
11420.0	60-65	15-20	3-5	3-5	TR-1	W	ID
11420.0	20-25	50-55	1-3	3-5	TR-1	W	IA, ID
11419.0	15-20	55-60	5-10	TR	TR-1	P	IIB
11415.0	40-45	20-25	10-15	1-5	0	PW	ID, IIB, ID
11415.0	30-35	25-30	20-25	1-3	TR	W	IIB, ID
11413.0	35-40	20-25	5-10	1-5	1-5	WP	IIB
11413.0	15-20	40-45	5-10	3-5	0	P/G	IIB
11411.5	5-30	25-30	5-10	1-5	0	PW	IBD, IF, IIB
11409.0	15-20	15-20	1-3	5-10	TR	WP	ICD, IIB, IIC
11407.0	25-30	45-50	3-5	TR-1	0	PW	IAC, ICD, IA, IBD,
11407.0	3-5	55-60	10-15	TR-1	0	PW	IF
11407.0	20-25	40-45	3-5	1-3	1-3	PW	I, IAD
11406.5	40-45	25-30	3-5	3-5	3-5	PW	NA
11406.0	10-15	50-55	10-15	3-5	1-3	P	IIB
11404.5	65-70	5-10	3-5	3-5	TR-1	M	IIA
11403.0	10-15	10-15	45-50	TR	0	M	IAB, ICD
11403.0	35-40	3-5	50-55	TR	0	M	IIB

THIN SECTION DESCRIPTIONS

1	2	3	4	5	6	7	8
NDGS# 2010							
8044.0	50-55	5-10	20-25	5-10	TR-1	M	ID
8031.9	65-70	10-15	5-10	TR-1	0	W	IIB
8031.9	50-55	10-15	10-15	TR-1	0	W	IB, ID, IIB
8031.8	60-65	5-10	5-10	0	0	W	ICD, IIB
8030.0	25-30	20-25	5-10	5-10	0	W	IIC, IIB
8029.0	35-40	15-20	15-20	TR-1	0	W	IIB
8028.0	25-30	10-15	5-10	1-3	TR-1	W	IIB
NDGS# 2967							
10587.0	55-60	15-20	10-15	TR-1	0	PW	IIC, IIA
10587.0	35-40	20-25	15-20	5-10	0	PW	IIB
10587.0	55-60	15-20	5-10	TR	0	PW	IIAB
10586.0	50-55	20-25	5-10	3-5	0	P	IIB
10585.5	55-60	10-15	5-10	TR-1	0	PW	IA, IIAB
10585.0	60-65	10-15	5-10	3-5	TR	W	IIB
10584.0	40-45	25-30	5-10	1-3	0	W	ID, IIB
10584.0	40-55	20-40	TR-15	0	0	W/P	IA, IIB
10584.0	45-50	25-30	10-15	TR-1	0	PW	ICD, IIB
10576.0	15-20	20-25	35-40	TR	TR-1	W	IIB
10576.0	56-70	3-5	10-15	TR	0	M	IIB
10566.0	75-80	5-10	1-3	1-3	0	M	IIB
10565.0	40-45	30-35	TR-1	3-5	0	W	IC
10565.0	55-60	15-20	TR-1	1-3	0	W	ID
10565.0	45-50	15-20	TR	1-3	TR	W	ICD
10563.0	25-30	40-45	TR-1	5-10	0	W	ICD
10563.0	25-30	30-35	3-5	3-5	TR	W	ID, ICD, IIB
10554.0	25-30	45-50	3-5	3-5	TR-1	P	IIB
10554.0	10-15	45-50	5-10	5-10	TR-1	P	IIA, IIB
10550.0	70-75	15-20	0	1-3	0	W	IIA
10550.0	75-80	5-10	0	3-5	0	W	IIA
10544.0	25-30	35-40	10-15	1-3	1-3	P	IIB
10544.0	5-10	30-35	20-25	20-25	0	W	IAC, ID
10541.5	0	0	0	90-95	0	DA	NA
10541.5	TR	3-5	0	90-95	0	DA	NA
NDGS# 2887							
9253.0	25-30	15-20	25-30	1-3	0	W	ID
9253.0	35-40	25-30	10-15	5-10	0	W	NA
9253.0	45-50	25-30	10-15	1-3	0	PW	ICD
9244.0	30-35	25-30	20-25	3-5	0	PW	IIBC
9235.0	50-55	10-15	10-15	3-5	0	W	IIB
9235.0	50-55	15-20	10-15	TR-1	TR	W	IIBC
9235.0	45-50	20-25	10-15	3-5	0	W	IIBC

THIN SECTION DESCRIPTIONS

1	2	3	4	5	6	7	8
9234.0	25-30	35-40	15-20	0	0	WP	IIB, IIC
9227.0	15-20	20-25	15-20	10-15	TR	W	IIB
9227.0	30-35	15-20	5-10	10-15	0	W	ID, IIB
9227.0	40-45	30-35	5-10	0	1-3	PW	ICD, IIB
9222.0	20-25	30-35	15-20	TR-1	TR	W	IIB
9222.0	40-45	20-25	10-15	TR	TR	W	IAC, IIB
9220.0	40-45	25-30	3-5	TR	0	PW	IB, IIB
9217.5	35-40	25-30	5-10	0	0	P	ICD, IIBC
9217.0	15-20	30-35	30-35	1-3	TR	PW	IA, IIB
9217.0	35-40	30-35	10-15	1-3	TR-1	P	IIB
9208.0	20-25	30-35	20-25	0	0	W	IAB, IIB
9207.0	35-40	20-25	10-15	TR	TR	W	IIB
9202.0	25-30	5-10	45-50	TR	0	M	NA
9202.0	5-10	10-15	50-55	0	0	W	IIB
9200.0	40-45	35-40	0	1-3	0	WP	IIBC, IIA
9198.0	30-35	50-55	0	1-3	0	P	ICD
9198.0	20-25	40-45	TR-1	3-5	TR	P	ICD
9198.0	20-25	40-45	0	10-15	TR	P	IC, IB

NDGS# 3086

10564.0	60-65	10-15	5-10	0	0	W	ID, IIB
10564.0	35-40	10-15	15-20	TR	0	W	IIC, IIBC
10559.0	35-40	30-35	15-20	0	0	PW	NA
10559.0	40-45	25-30	15-20	TR	0	P	IIB
10559.0	45-50	30-35	5-10	0	0	PW	IC
10558.0	70-75	10-15	1-3	1-3	0	W	IC, IIB
10558.0	80-85	3-5	1-3	TR-1	0	M	ID, IIBC
10557.5	55-60	15-20	10-15	0	0	W	IIB
10553.5	20-25	15-20	45-50	0	0	W	IBD, IIB
10551.5	35-40	20-25	25-30	TR	0	W	IA, IIB
10551.0	30-35	20-25	25-30	3-5	0	W	IIB
10551.0	50-55	15-20	10-15	5-10	0	W	IAB, IIB
10550.0	55-60	10-15	15-20	TR	0	W	ID, IIB
10550.0	55-60	15-20	5-10	0	0	PW	IACD
10544.0	35-40	20-25	15-20	0	TR	W	IIB
10541.0	25-30	30-35	20-25	TR	TR	W	IIB
10540.0	10-20	45-50	25-30	0	TR-1	B	IIB
10538.0	10-20	40-45	25-30	1-3	TR-1	W	ID
10535.0	25-30	45-50	5-10	3-5	0	B	ID, IAC
10524.5	5-10	75-80	3-5	TR	TR-1	P	ID
10521.0	40-45	40-45	3-5	0	1-3	WP	IAB, IIA
10520.5	45-50	35-40	3-5	TR	1-3	WP	ID
10515.5	50-55	20-25	5-10	3-5	0	PW	ID, IIB
10515.0	50-55	20-25	3-5	3-5	TR	PW	ICD, IIB
10515.0	35-40	20-25	3-5	1-3	TR	W	ID

THIN SECTION DESCRIPTIONS

1	2	3	4	5	6	7	8
10515.0	30-35	30-35	5-10	10-15	0	P	ID
10514.0	0	70-75	3-5	0	3-5	B	IC
10513.7	30-35	40-45	TR-1	3-5	1-3	P	NA
10511.0	30-35	10-15	15-20	10-15	0	DW	ICD
10511.0	35-40	15-20	5-10	10-15	0	PW	IICD
10511.0	25-30	15-20	15-20	10-15	0	W	ICD
10510.0	0	0	25-30	65-70	0	DA	NA
10509.5	10-15	5-10	35-40	30-35	0	DA	ID
10509.0	10-15	0	55-60	15-20	0	M	IA, IDC
10509.0	5-10	10-15	30-35	35-40	0	DA	ID
10509.0	TR-1	0	25-30	65-70	0	DA	IB
10507.5	TR	0	15-20	75-80	0	DA	NA
10507.5	0	0	25-30	60-65	0	DA	NA
10507.5	0	0	35-40	55-60	0	DA	NA
10507.0	0	0	55-60	35-40	0	DA	NA

NDGS# 2602

10087.0	15-20	25-30	30-35	TR-1	1-3	WP	IIB
10077.0	30-35	40-45	5-10	1-3	TR	B	IAC, IIA
10076.5	20-25	45-50	3-5	5-10	0	B	ID
10076.0	60-65	10-15	TR-1	10-15	TR-1	W	IACD
10076.0	70-75	3-5	TR-1	10-15	0	M	ID
10075.0	60-65	5-10	1-3	3-5	TR-1	M	ID
10074.0	60-65	15-20	TR-1	1-3	TR	W	ID
10074.0	75-80	3-5	0	5-10	0	M	NA
10065.0	60-65	10-15	5-10	3-5	TR-1	W	IIAB
10063.5	15-20	40-45	15-20	3-5	3-5	P	IIB
10059.0	5-10	50-55	15-20	0	3-5	P	IIB
10045.0	0	0	50-55	35-40	0	DA	NA
10041.0	0	0	55-60	25-30	0	DA	NA

NDGS# 6642

10869.0	40-45	15-20	15-20	3-5	0	PW	ICD, IIB
10869.0	20-25	15-20	35-40	0	0	PW	IIB
10861.5	5-10	10-15	65-70	0	TR-1	D	NA
10859.0	40-45	15-20	25-30	TR-1	0	W	ICD, IIA
10859.0	20-25	15-20	25-30	3-5	0	W	IABCD
10851.5	30-35	15-20	10-15	3-5	0	W	IIB
10851.5	30-35	30-35	3-5	1-3	0	PW	ICD
10851.5	25-30	30-35	10-15	5-10	0	WP	ICDB, IIB
10850.0	5-10	10-40	15-50	5-15	0	P	ICD
10845.0	10-15	30-35	5-10	10-15	0	P	ID
10845.0	15-20	30-35	10-15	10-15	0	P	IAC

THIN SECTION DESCRIPTIONS

1	2	3	4	5	6	7	8
10840.5	5-10	50-55	0	30-35	0	B	IIB, IIC
10839.0	0	55-60	0	25-30	0	B	ID
10837.0	0	40-45	0	45-50	0	DA	IIB
10837.0	0	60-65	0	25-30	0	DA	IIB
10837.0	0	55-60	0	30-35	0	B	IIB
10815.5	30-35	0	55-60	0	0	M	IAB
10810.5	15-20	55-60	0	3-5	0	P	IAB
10810.5	20-25	30-35	0	20-25	0	WP	ID
10801.5	40-45	1-3	40-45	TR	1-3	M	NA

APPENDIX B

MORPHOLOGIC DATA OF STYLOLITES

Appendix B contains the results of the measurement of amplitudes and wavelengths of the stylolites in the studied section. The measurements are divided by wells. The first column labeled "DEPTH" gives the depth of the measurement. The A1, A2 and A3 columns are the size (in millimetres) of the amplitudes measured. The W1, W2 and W3 columns are the sizes (in millimetres) of the corresponding wavelengths. The columns "TN" and "TK" are the minimum and maximum thickness, respectively, of the stylolite seam within the measure interval.

MORPHOLOGIC DATA OF STYLOLITES

DEPTH	A1	A2	A3	W1	W2	W3	TN	TK
-------	----	----	----	----	----	----	----	----

NDGS# 286

4105.0	0.030	0.030	0.030	2.250	0.630	0.300	0.015	0.120
4102.5	0.030	0.030	0.015	0.450	0.300	0.180	0.015	0.060
4098.0	0.600	0.540	1.200	0.720	1.500	0.510	0.015	0.090
4097.0	0.300	0.060	0.060	0.660	0.150	0.120	0.015	0.120
4069.0	0.330	0.150	0.270	0.900	0.960	0.300	0.060	0.150

NDGS# 999

11284.0	0.060	0.060	0.030	0.930	0.240	0.270	0.030	0.060
11257.0	0.150	0.030	0.060	0.150	0.150	0.300	0.015	0.030

NDGS# 4599

7508.0	1.800	1.380	1.140	1.920	0.600	1.860	0.015	0.360
7506.0	0.750	0.510	0.840	0.630	0.330	1.050	0.015	0.030
7503.0	0.060	0.030	0.060	0.210	0.225	0.180	0.015	0.015
7502.5	0.390	0.600	1.050	0.330	0.840	2.670	0.060	0.150
7501.0	1.200	0.390	0.510	1.200	0.960	0.450	0.015	0.030
7501.0	1.500	0.600	2.400	4.200	1.440	3.000	0.030	0.240
7499.5	0.360	0.270	0.390	1.350	0.150	0.150	0.060	0.270
7495.0	0.630	0.150	0.270	0.750	0.720	0.780	0.060	0.300
7490.6	0.120	0.030	0.030	0.150	0.150	0.120	0.030	0.030
7490.0	0.120	0.090	0.420	0.390	0.090	0.300	0.030	0.045
7489.0	0.270	0.060	0.060	0.900	0.570	1.800	0.030	0.120
7489.0	0.240	0.090	0.090	0.420	0.570	0.090	0.015	0.060
7486.0	0.960	0.690	0.690	0.600	0.810	0.840	0.015	0.090
7486.0	0.060	0.090	0.060	0.900	0.390	0.180	0.030	0.075
7465.5	0.540	0.450	0.360	0.660	0.450	0.420	0.015	0.090
7465.5	0.060	0.090	0.060	0.900	0.390	0.180	0.030	0.750
7465.0	0.090	0.060	0.060	0.180	0.270	0.240	0.030	0.060

NDGS# 38

5554.5	0.060	0.150	0.060	0.180	0.150	0.240	0.030	0.060
5553.0	0.210	0.630	0.600	1.800	1.200	1.260	0.030	0.090
5546.0	0.510	0.120	0.090	0.120	0.210	0.240	0.030	0.060
5506.0	0.030	0.030	0.030	0.840	1.140	0.600	0.060	0.090

MORPHOLOGIC DATA OF STYLOLITES

DEPTH	A1	A2	A3	W1	W2	W3	TN	TK
NDGS# 2828								
11420.0	0.660	0.270	0.360	1.020	0.330	0.510	0.015	0.090
11420.0	0.090	0.120	0.030	0.420	0.540	0.240	0.015	0.060
11419.0	0.180	0.210	0.060	0.240	0.360	0.210	0.030	0.060
11415.0	0.360	0.150	0.090	0.300	0.180	0.150	0.015	0.030
11415.0	0.030	0.060	0.090	0.330	0.120	0.210	0.015	0.030
11409.0	0.270	0.090	0.060	0.270	0.060	0.120	0.015	0.030
11403.0	0.750	0.060	1.200	0.600	3.000	1.920	0.030	0.150
NDGS# 2010								
8044.0	0.060	0.060	0.150	0.150	0.270	0.240	0.015	0.030
8031.9	0.180	0.240	0.150	1.020	0.750	0.900	0.030	0.030
8031.9	0.022	0.044	0.044	0.099	0.099	0.066	0.001	0.011
8031.8	0.120	0.090	0.150	0.300	0.420	0.840	0.030	0.150
8029.0	0.210	0.090	0.060	0.870	0.330	0.270	0.030	0.060
NDGS# 2967								
10584.0	0.630	0.150	0.030	0.750	0.390	0.600	0.011	0.022
10584.0	2.910	0.900	4.350	1.440	1.350	5.250	0.008	0.360
10576.0	0.060	0.150	0.090	0.270	0.840	0.300	0.011	0.030
10565.0	0.022	0.022	0.055	0.187	0.088	0.176	0.004	0.008
10563.0	0.060	0.060	0.210	0.210	0.150	0.210	0.030	0.030
10563.0	0.060	0.060	0.120	0.270	0.540	0.510	0.011	0.022
10550.0	0.420	0.330	0.150	0.270	0.390	0.510	0.001	0.011
10544.0	0.300	0.210	0.090	0.390	0.450	0.300	0.030	0.060
NDGS# 2887								
9253.0	0.240	0.600	0.960	0.570	0.240	0.270	0.011	0.750
9244.0	0.150	0.060	0.090	0.420	0.690	0.420	0.030	0.060
9235.0	0.090	0.090	0.060	0.150	0.240	0.150	0.011	0.033
9234.0	0.044	0.055	0.022	0.176	0.066	0.055	0.011	0.022
9227.0	0.240	0.030	0.030	0.510	0.270	0.210	0.055	0.088
9222.0	0.630	0.870	0.120	0.540	0.420	0.330	0.011	0.030
9217.0	0.022	0.022	0.044	0.055	0.132	0.231	0.011	0.022
9208.0	1.020	0.960	0.900	0.960	0.690	0.660	0.011	0.060
9207.0	0.033	0.011	0.033	0.066	0.088	0.077	0.011	0.011

MORPHOLOGIC DATA OF STYLOLITES

DEPTH	A1	A2	A3	W1	W2	W3	TN	TK
9200.0	0.022	0.033	0.022	0.198	0.099	0.099	0.011	0.022
9198.0	0.240	0.720	0.180	1.110	0.750	0.690	0.011	0.075
9198.0	0.060	0.150	0.210	0.210	0.630	0.750	0.030	0.090
9198.0	0.066	0.044	0.077	0.099	0.143	0.165	0.011	0.033

NDGS# 3086

10564.0	0.099	0.033	0.011	0.198	0.088	0.055	0.004	0.008
10559.0	0.044	0.044	0.022	0.077	0.066	0.066	0.004	0.008
10558.0	0.060	0.060	0.210	0.240	0.180	0.750	0.008	0.030
10558.0	0.060	0.060	0.120	0.180	0.240	0.150	0.008	0.011
10553.5	0.300	0.150	0.120	0.570	0.270	0.330	0.045	0.060
10551.0	4.650	3.570	2.550	1.590	1.620	1.830	0.004	0.180
10550.0	0.033	0.033	0.033	0.132	0.055	0.066	0.004	0.012
10550.0	0.840	0.750	0.120	1.050	1.200	0.360	0.011	0.060
10540.0	0.120	0.090	0.060	0.240	0.450	0.450	0.022	0.066
10538.0	0.033	0.022	0.055	0.099	0.088	0.077	0.011	0.011
10535.0	0.022	0.022	0.011	0.132	0.033	0.044	0.000	0.008
10524.5	0.090	0.150	0.210	0.420	0.540	0.330	0.011	0.033
10521.0	3.900	5.100	1.590	2.700	1.560	0.900	0.030	0.120
10520.5	0.150	0.300	0.180	0.300	0.180	0.360	0.011	0.033
10515.5	0.011	0.033	0.022	0.088	0.110	0.088	0.004	0.011
10515.0	0.060	0.120	0.240	0.390	0.690	0.510	0.011	0.033
10515.0	0.099	0.044	0.055	0.121	0.077	0.088	0.002	0.004
10511.0	0.300	0.210	0.090	0.900	0.300	0.150	0.004	0.011
10511.0	0.044	0.044	0.088	0.099	0.055	0.077	0.008	0.011
10511.0	0.090	0.060	0.240	0.270	0.420	0.420	0.004	0.011
10509.5	0.055	0.066	0.044	0.110	0.110	0.099	0.011	0.011
10509.0	3.750	2.100	1.800	3.900	5.200	1.800	0.008	0.150
10509.0	0.420	0.480	0.090	1.500	0.720	0.750	0.030	0.150

NDGS# 2602

10087.0	0.033	0.011	0.011	0.187	0.198	0.033	0.004	0.010
10076.0	0.033	0.033	0.044	0.099	0.077	0.044	0.004	0.011
10076.0	0.150	0.150	0.030	0.300	0.330	0.240	0.030	0.090
10075.0	0.121	0.077	0.022	0.253	0.099	0.132	0.011	0.033
10074.0	0.030	0.060	0.090	0.090	0.240	0.210	0.008	0.011

MORPHOLOGIC DATA OF STYLOLITES

DEPTH	A1	A2	A3	W1	W2	W3	TN	TK
NDGS# 6642								
10869.0	0.270	0.120	0.210	0.270	0.240	0.210	0.011	0.033
10859.0	0.270	0.450	1.080	0.720	0.600	1.380	0.030	0.300
10859.0	0.090	0.210	0.060	0.300	0.300	0.150	0.002	0.022
10851.5	0.150	0.210	0.060	0.390	0.270	0.120	0.004	0.033
10851.5	0.330	0.090	0.150	0.540	0.210	0.150	0.011	0.011
10850.0	0.450	0.300	0.360	0.600	1.500	1.650	0.030	0.510
10845.0	0.870	0.180	1.200	0.900	9.900	1.260	0.022	0.180
10840.5	2.700	1.050	0.690	9.090	2.670	2.700	0.120	0.810
10839.0	0.120	0.060	0.030	0.210	0.150	0.120	0.011	0.022
10837.0	0.060	0.030	0.030	0.330	0.240	0.360	0.001	0.003
10815.5	1.500	1.500	3.330	1.950	2.730	5.100	0.030	1.350
10810.5	0.210	0.120	0.030	0.150	0.120	0.090	0.004	0.011

APPENDIX C

CHEMICAL DATA FOR REACTATE DOLOMITES

This appendix contains the electron microprobe analyses for selected reactate dolomites from the studied section. The first columns numbered 1 through 6 list the chemical data by weight percent of the oxide shown. The last two columns, 7 and 8, show the cation proportion for calcium and magnesium.

CHEMICAL DATA FOR REACTATE DOLOMITES

1	2	3	4	5	6	7	8
CAO	MGO	FEO	MNO	SIO2	SO3	CA	MG
NDGS# 2828, DEPTH 11415 feet below KB							
28.1	19.0	0.00	0.04	0.07	0.00	1.03	0.97
28.1	18.9	0.08	0.00	0.10	0.09	1.03	0.96
28.3	18.0	0.00	0.00	0.11	0.06	1.06	0.94
28.6	19.8	0.00	0.06	0.10	0.13	1.02	0.98
28.7	18.6	0.05	0.00	0.00	0.08	1.05	0.95
28.9	18.2	0.12	0.03	0.16	0.18	1.06	0.93
28.8	18.9	0.00	0.00	0.00	0.11	1.04	0.95
NDGS# 2887, DEPTH 9217 feet below KB							
28.7	19.4	0.00	0.06	0.21	0.11	1.03	0.97
29.5	19.9	0.04	0.00	0.00	0.10	1.03	0.97
29.1	19.3	0.18	0.00	0.43	0.15	1.03	0.95
28.0	17.5	0.11	0.00	0.10	0.00	1.07	0.93
28.7	16.2	0.06	0.00	0.00	0.00	1.12	0.88
29.1	18.9	0.05	0.05	0.07	0.18	1.05	0.94
29.6	50.0	0.11	0.06	0.15	0.07	1.03	0.96
9.9	19.8	0.19	0.00	0.09	0.00	1.04	0.96
NDGS# 3086, DEPTH 10515.5 feet below KB							
30.0	19.6	0.15	0.00	0.13	0.09	1.04	0.95
30.0	19.5	0.18	0.00	0.27	0.13	1.04	0.94
29.9	19.7	0.19	0.00	0.07	0.05	1.07	0.93
29.5	19.4	0.76	0.07	0.48	1.59	1.01	0.92
30.2	19.8	0.11	0.00	0.10	0.08	1.04	0.95
30.0	18.3	0.12	0.00	0.25	0.07	1.06	0.93
30.0	22.3	0.11	0.03	0.26	0.00	0.98	1.01
29.7	24.4	0.20	0.05	0.31	0.11	0.93	1.06
NDGS# 6642, DEPTH 10851.5 feet below KB							
29.7	21.5	0.23	0.00	0.66	0.09	0.98	0.99
29.8	21.9	0.23	0.05	0.32	0.14	0.98	1.00
29.4	19.5	0.06	0.07	0.26	0.05	1.04	0.95
29.9	20.7	0.08	0.04	0.00	0.09	1.02	0.98
30.5	24.2	0.00	0.08	0.11	0.05	0.95	1.05
31.2	22.2	0.08	0.00	0.00	0.05	0.99	1.01
30.1	23.5	0.21	0.00	0.26	0.09	0.95	1.04

REFERENCES CITED

- Bathurst, R.G.C., 1958, Diagenetic fabrics in some British Dinantian limestones: *Liverpool Manchester Geological Journal*, v. 2, p. 11-36.
- Bathurst, R.G.C., 1975, *Developments in sedimentology 12, carbonate sediments and their diagenesis*, Elsevier Scientific Publishing Company, 658 p.
- Bence, A.E., and Albee, A., 1968, Empirical correction factors for electron microanalysis of silicates and oxides: *Journal of Geology*, v. 76, p. 380-403.
- Berner, R.A., 1980, *Early diagenesis, a theoretical approach*, Princeton University Press, Princeton, N.J., 241 p.
- Buxton, T.M., and Sibley, D.F., 1981, Pressure solution features in a shallow buried limestone: *Journal of Sedimentary Petrology*, v. 51, p. 19-26.
- De Boer, 1977, On the thermodynamics of pressure solution-interaction between chemical and mechanical forces: *Geochimica et Cosmochimica Acta*, v. 41, p. 249-256.
- Dunham, R.J., 1962, classification of carbonate rocks according to depositional texture: in W.E. Ham, ed., *Depositional Environments in Carbonate Rocks: American Association of Petroleum Geologists Memoir 1*, p. 108-121.
- Dunnington, H.V., 1954, Stylolite development post-dates rock induration: *Journal of Sedimentary Petrology*, v. 24, no.1, p. 27-49.
- Fasciolas, A.E., and Powell, T.G., 1978, Mineralogical and geochemical transformation of clays during burial diagenesis (catagenesis): relation to oil generation: in Mortland, M.M., and Farmer, V.C., eds. *International Clay Conference 1978*, Elsevier Scientific Publishing Co., Amsterdam, p. 261-270.
- Folk, R.L., 1974, The natural history of crystalline calcium carbonate: effect of magnesium content and salinity: *Journal of Sedimentary Petrologists*, v. 44, p. 40-53, Figs. 1-9.
- Gaines, A.M., 1980, Dolomitization Kinetics: recent experimental studies: in Zenger, D.H., Dunham, J.B., and Ethington, R.L., eds., *Concepts and Models of Dolomitization: Society of Economic Paleontologists Mineralogists Special Publication 28*, p. 81-86.

- Given, R.K., and Wilkinson, B.H., 1985, Kinetic control of morphology, composition, and mineralogy of abiogenic sedimentary carbonates: *Journal of Sedimentary Petrology*, v. 55, p. 109-119.
- Gregg, J.M., and Sibley, D.F., 1984, Epigenetic dolomitization and the origin of xenotopic dolomite texture: *Journal of Sedimentary Petrology*, v.54, p. 908-931.
- Goldstein, J.I., Newbury, D.E., Echlin, P., Joy, D.C., Fiori, C., Lifshin, E., 1984, Scanning electron microscopy and x-ray microanalysis, Plenum Press, New York, 673 p.
- Jenkins, R., 1974, An introduction to x-ray spectrometry, Heyden, London, 162 p.
- Jorgensen, N.O., 1983, Dolomitization in chalk from the North Sea central graben: *Journal of Sedimentary Petrology*, v. 53, p. 557-564.
- Kahle, C.F., 1965, Possible roles of clay minerals in the formation of dolomite: *Journal of Sedimentary Petrology*, v. 35, p. 448-453.
- Krauskopf, K.B., 1979, Introduction to geochemistry, McGraw-Hill Book Company, New York, New York, 617 p.
- Loeffler, P.T., 1982, Depositional environment and diagenesis, Birdbear Formation (upper devonian), Williston Basin, North Dakota: M.S. Thesis, University of North Dakota, 268 p., unpublished.
- Logan, B.W., and Semeniuk, V., 1976, Dynamic metamorphism; processes and products in Devonian carbonate rocks, Canning Basin, Western Australia: Webby, B.W., ed., Geological Society of Australia Special Publication No.6, 138 p.
- Mattes, B.W., and Mountjoy, E.W., 1980, Burial dolomitization of the upper Devonian Miette buildup, Jasper National Park, Alberta: Society of Economic Paleontologist Mineralogist Special Publication No. 28, p. 259-297.
- McHargue, T.R. and Price, R.C., 1982, Dolomite from clay in argillaceous or shale-associated marine carbonates: *Journal of Sedimentary Petrology*, v. 52, p. 876-886.

- Schmidt, G.W., 1973, Interstitial water composition and geochemistry of deep Gulf Coast shales and sandstones: American Association of Petroleum Geologists Bulletin, v. 57, p. 321-337.
- Shinn, E.A., and Robbin, D.M., 1983, Mechanical and chemical compaction in fine-grained shallow-water limestones: Journal of Sedimentary Petrology, v. 53, p. 595-618.
- Sibley, D.F., 1982, The origin of common dolomite fabrics: clues from the Pliocene: Journal of Sedimentary Petrology, v. 52, p. 1087-1100.
- Sibley, D.F., and Gregg, J.M., 1987, Classification of dolomite rock textures: Journal of Sedimentary Petrology, v. 57, p. 967-975.
- Stockdale, P.B., 1923, Stylolites-their nature and origin: Indiana University Studies, no.9, 97 p.
- Stockdale, P.B., 1943, Stylolites: Primary or secondary: Journal of Sedimentary Petrology, v. 13, p. 3-12.
- Sorby, H.C., 1879, On the structure and origin of limestones: Quarterly Journal, Geological Society of London, v. 35, p. 56-95.
- Wanless, H.R., 1979, Limestone response to stress: pressure solution and dolomitization: Journal of Sedimentary Petrology, v. 49, p. 437-462.
- Weyl, P.K., 1959, Pressure solution and the force of crystallization--a phenomenological theory: Journal of Geophysical Research, V. 64, p. 2001-2025.